Biogeosciences, 23, 2431–2450, 2026
https://doi.org/10.5194/bg-23-2431-2026

Biogeosciences Open Access EGU

Temporary waterlogging alters CO_2 flux dynamics but not cumulative emissions in cultivated mineral soils

Reija Kronberg[1,2], Sanna Kanerva[1], Markku Koskinen[1,2], Tatu Polvinen[1,2], Tuomas Mattila[3], and Mari Pihlatie[1,2]

[1]Department of Agricultural Sciences, Unit of Environmental Soil Science, University of Helsinki, Viikinkaari 9, P.O. Box 56, 00014 Helsinki, Finland
[2]Institute for Atmospheric and Earth System Research (INAR)/Faculty of Agriculture and Forestry, University of Helsinki, Viikinkaari 9, P.O. Box 56, 00014 Helsinki, Finland
[3]Finnish Environment Institute SYKE, Latokartanonkaari 11, 00790, Helsinki, Finland

Correspondence: Reija Kronberg (reija.kronberg@helsinki.fi) and Mari Pihlatie (mari.pihlatie@helsinki.fi)

Received: 12 June 2025 – Discussion started: 8 July 2025
Revised: 25 March 2026 – Accepted: 30 March 2026 – Published: 13 April 2026

Abstract. Increasingly variable rainfall patterns expose soils to more frequent waterlogging in humid climates. Yet, the effects of waterlogging on soil organic matter decomposition in mineral soils remain uncertain. We studied the impact of off-season waterlogging on carbon dioxide (CO_2) production and dissolved carbon dynamics in controlled greenhouse conditions using 32 monolithic soil columns (hereafter monoliths) ($h = 63$ cm, $d = 15.2$ cm) sampled from two agricultural fields (silty clay, sandy loam) in southern Finland. The 1.5 year study comprised three growth cycles with alternating growing and off-seasons. Spring barley (*Hordeum vulgare*) was grown in all monoliths during the growing seasons. In turn, during all three off-seasons, half of the monoliths were subjected to waterlogging lasting seven weeks, while in the other half soil moisture was maintained at $\sim 70\%$ field capacity. Within these water treatment groups (waterlogged and control), the monoliths were further divided into two plant treatment groups: in half of the monoliths, an overwintering cover crop (*Festuca arundinacea*) was grown, while in the other half soil was left bare for the off-seasons. Soil temperature and moisture were continuously monitored, dissolved organic (DOC) and inorganic carbon (DIC) concentrations in pore water were analyzed at three depths and CO_2 fluxes were measured at the surface. Contrary to our hypothesis, waterlogging did not increase soil DOC content. Instead, on-going microbial/rhizospheric activity promoted an increase in DIC content while CO_2 fluxes declined, indicating an accumulation of respired CO_2 in soil pore water. The sustained CO_2 production could not be explained solely by mobilization of Fe-associated C, as initially hypothesized. After the onset of drainage of the waterlogged monoliths, CO_2 fluxes from both soils increased more than predicted based on changes in soil moisture and temperature, likely due to the release of previously accumulated CO_2. These post-waterlogging increases in CO_2 fluxes roughly equaled the earlier decreases during waterlogging. Thus, although off-season waterlogging strongly influenced the temporal dynamics of CO_2 fluxes, it did not alter total cumulative CO_2 emissions from the studied agricultural soils.

1 Introduction

Climate change is causing significant alterations in rainfall patterns globally by increasing the inter- and intra-seasonal variability, and intensifying the climatic extremes (IPCC, 2023). In humid boreal regions, mild and rainy winters may lead to prolonged and more frequent soil waterlogging outside growing seasons (Mattila and Vihanto, 2024; Ruosteenoja and Jylhä, 2022). Soil moisture is a critical environmental factor influencing soil carbon (C) fluxes (Raich and Schlesinger, 1992). Yet, uncertainties remain concerning the response of soil organic matter (OM) decomposition and carbon dioxide (CO_2) efflux to relatively short periods of very high soil moisture (weeks to a few months; i.e. temporary waterlogging) in cultivated mineral soils (Fairbairn et al., 2023; Ghezzehei et al., 2019; Goffin et al., 2015; Huang and Hall, 2017; Moyano et al., 2018). Deepening our un-

derstanding of the relationship between soil moisture and C dynamics at or near complete soil water saturation with potentially anaerobic conditions is crucial for improving predictions of soil-climate feedbacks in changing environmental conditions.

Contrary to conventional theory, recent studies suggest that temporary anaerobic conditions may maintain or even increase total C mineralization in mineral soils, relative to static aerobic conditions (e.g. Huang et al., 2021; Huang and Hall, 2017; Liu et al., 2023; Winkler et al., 2019). Although many C cycling and respiration models still predict near zero CO_2 fluxes at water saturation (Ghezzehei et al., 2019; Moyano et al., 2013; Sulman et al., 2014), mineral soils have been shown to sustain substantial CO_2 production in these conditions due to on-going anaerobic respiration (Fairbairn et al., 2023; Huang et al., 2021; Huang and Hall, 2017; Liu et al., 2023; Moyano et al., 2018; Wickland and Neff, 2008; Zheng et al., 2019). This occurs because most of the OM is stabilized by mineral associations (Salonen et al., 2024; von Lützow et al., 2007) which provides protection against biodegradation (Cotrufo et al., 2019; Lavallee et al., 2020), at least in static oxic conditions. In humid soils, redox active iron(III) (Fe(III)) (hydr)oxides represent essential binding agents (Aasano et al., 2018; Rasmussen et al., 2018; Torn et al., 1997). Therefore, if soil saturates with water for prolonged periods and reducing conditions form in the bulk soil, (facultative) anaerobic microbes start utilizing alternative terminal electron acceptors (TEA), such as Fe(III) oxides, instead of oxygen (O_2), to oxidize OM (Fiedler et al., 2007; Jakobsen et al., 1981; Peters and Conrad, 1996; Ponnamperuma, 1985). Upon reduction, the solubility of Fe increases, which leads to the disruption of Fe oxides and the release of OM associated with them, thereby making OM vulnerable to mineralization (Chen et al., 2020; Fairbairn et al., 2023; Grybos et al., 2009; Huang et al., 2021, 2020; Huang and Hall, 2017).

The influence of anaerobic conditions on C mineralization has, however, not been uniform across soils and experiments. Soil characteristics, such as texture, the amount (Hanke et al., 2013; Liu et al., 2023; Winkler et al., 2019; Zhao et al., 2020) and reducibility (Ginn et al., 2017) of active Fe oxides, and the availability of labile C substrates (e.g. Winkler et al., 2019), influence the soil's response to waterlogging. Naturally, an adequate amount of reducible Fe that binds OM is a prerequisite for increased OM vulnerability due to Fe reduction. Although in humid boreal soils Fe oxides represent a minority of the clay-sized fraction (Ito and Wagai, 2017), amorphous, low-crystallinity forms constitute a substantial component of the oxide pool (Keskinen et al., 2022; Sippola 1974). In the soils studied here, for example, short-range-ordered (SRO) Fe oxides represent $\sim 50\,\%$ of all pedogenic Fe (Kronberg et al., 2024). Generally, SRO Fe and Al oxides play a disproportionately important role in C stabilization thanks to their high specific surface area and chemical reactivity (Kaiser and Guggenberger, 2003; Yong et al., 1992). Moreover, naturally occurring oscillations in soil oxygen availability, particularly in fine-textured humid soils, may enhance Fe reducibility (Ginn et al., 2017) thereby eventually also influencing C availability. Indeed, a recent large-scale study of arable soils in southern Finland showed that Fe oxides correlated with mineral-associated organic C, particularly in soils with high clay contents (Salonen et al., 2024). However, to our knowledge, studies focusing on Fe–OM interactions in agricultural boreal soils under temporary anoxia are lacking, and it therefore remains unknown whether and how seasonal waterlogging affects C dynamics in these systems. Because soil redox reactions are predominantly microbially catalyzed (Sigg, 2000; Stumm, 1995), the availability of labile C substrates stimulates microbial activity and O2 consumption, thereby promoting the formation of reducing conditions and associated Fe redox transformations (Khan et al., 2019; Muhammad et al., 2021; Winkler et al., 2019).

In natural and cultivated soils, roots are a source of readily degradable C for soil microbes (Kuzyakov, 2006; Muhammad et al., 2021). As much as half of the C photosynthetically fixed by plants can be allocated belowground (Chandregowda et al., 2023; Clemmensen et al., 2013; Keiluweit et al., 2015). In agriculture, the cultivation of overwintering cover crops has been recognized as an effective strategy to increase soil C inputs and thus, promote soil C sequestration (Kaye and Quemada, 2017; Poeplau and Don, 2015). However, it has also been observed that root exudates can stimulate decomposition of OM through priming (Bingeman et al., 1953), either directly by increasing microbial activity or indirectly by promoting the mobilization of C associated with soil minerals (Keiluweit et al., 2015; Kuzyakov et al., 2000). This, together with the changing climatic conditions, introduces complexity in assessing the net impact of cover crops on soil C dynamics (Jian et al., 2020; Poeplau and Don, 2015). To our knowledge, the impact of cover crops on C fluxes during periodic waterlogging has gained very little attention, despite the potential for root-derived C inputs to promote the mobilization of stable, mineral-associated C. Thus, it remains unknown whether and to what extent the labile C inputs from roots affect C dynamics in temporarily waterlogged conditions.

Thus far, studies focusing on the effects of water saturation/anaerobic conditions on OM mobilization and CO_2 fluxes in mineral soils have mainly been either laboratory incubations (Bhattacharyya et al., 2018; Fairbairn et al., 2023; Huang et al., 2021, 2020; Huang and Hall, 2017; Zhao et al., 2020) or field studies (Jeanneau et al., 2020; Possinger et al., 2020). Mesocosms allow assessing the role of soil structure and plant cover on C flows and transformations, while maintaining the control over environmental conditions, but so far they have been rarely used. In our 1.5 year greenhouse experiment, we studied C dynamics in intact soil profiles under controlled temperature and moisture to capture processes more representative of field conditions. The data used

in this study was collected from a soil monolith experiment which experimental procedure has been described in our preceding publication (Kronberg et al., 2024). In this particular study, we investigated how seasonal waterlogging affects CO_2 fluxes and dissolved C species dynamics in two hydrologically distinct cultivated mineral soil profiles (silty clay, sandy loam) with and without overwintering cover crop (Tall Fescue, *Festuca arundinacea*). Finally, an empirical model describing the dependency of soil respiration on temperature and moisture was fitted to the data to assess its ability to simulate observed CO_2 flux dynamics during and after waterlogging. The following hypotheses were set:

(a) Temporary waterlogging mobilizes Fe-associated C leading to increased soil DOC content during waterlogging.

(b) Temporary waterlogging does not reduce the total cumulative CO_2 emissions from either soil.

(c) Silty clay with higher OM, clay and Fe oxide contents result in higher cumulative CO_2 fluxes than from sandy loam soil.

(d) Soil C input from cover crops promotes C dissolution and CO_2 production in waterlogged conditions.

2 Material and methods

2.1 Soil monolith experiment

Cylindrical soil monoliths (d, 15.2 cm; h, 63 cm) were collected with a tractor-mounted soil auger (Uusitalo et al., 2012) in November 2020 and May 2021 from two agricultural fields in Southern Finland classified as Eutric Stagnosol (60°16′23.4″ N 24° 56′40.6″ E) and Eutric Cambisol/Mollic Umbrisol (60°49′07.3″ N 23°45′54.8″ E) with silty clay and sandy loam USDA texture, respectively. These soils represented typical OM (Fernandez-Ugalde et al., 2022; Heikkinen et al., 2013; Lemola et al., 2018) and SRO Fe oxide contents for the region. The two soils differed in their hydrological characteristics. The dense structure and fine texture in the silty clay soil limited the movement of water through the profile causing water stagnation and repeated alteration of oxidized and reduced conditions resulting in the formation of stagnic properties (see Kronberg et al., 2024). In contrast, the coarse texture in the sandy loam soil facilitated an efficient water movement and transport of solutes into deeper soil layers. In the profile brown colors indicated a release of Fe from primary minerals. Selected soil properties are presented in Table 1.

The experiment was established in a greenhouse compartment at University of Helsinki in June 2021, and it is described in detail in Kronberg et al. (2024). Briefly, 32 soil monoliths were collected from the two agricultural fields, with 16 from each soil type. These monoliths were assigned to a factorial design with two plant treatments and two water treatments. This setup resulted in eight unique treatment combinations (2 soil types × 2 plant treatments × 2 water treatments), each having four treatment replicates (Fig. 1). During the 1.5 year-long experiment, three study cycles with alternating growing and off-seasons were conducted. Repeated cycles were conducted to assess (i) whether the observed responses were consistent over study cycles, thereby increasing the robustness of our findings, and (ii) whether treatment effects, particularly those related to the cover crop, required time to emerge, given that measurable changes in soil properties develop gradually. Here, only the results from the second and the third study cycles are presented because the first cycle was dedicated for optimization of the experimental conditions, sampling and monitoring methods.

Soil temperature, volumetric water content (SVWC, $m^3\,m^{-3}$) and redox potential (E_h) were continuously measured at 10, 30 and 50 cm soil depths in three out of four replicated monoliths (24 in total). Soil temperature and SVWC were measured with Teros12 sensors (METER Group, USA). The soil moisture readings were calibrated to each monolith according to the gravimetric soil moisture content and bulk density determined at the end of the experiment (Kronberg et al., 2024). E_h was measured by platinum electrodes together with Ag/AgCl saturated KCl reference electrodes (Paleo Terra, The Netherlands). Data was logged with a Campbell datalogger (Campbell Scientific CR800 with two AM16/32B multiplexers) (Kronberg et al., 2024). The target seasonal temperatures (day/night) for the greenhouse were 20/15 °C for summer, 15/10 °C for autumn, 10/5 °C for winter and 15/10 °C for spring. The soil temperature was controlled with a separate cooler and an insulation box constructed around the soil monoliths. The realized mean soil temperature at 30 cm depth was 15.1 and 15.3 °C in summer, 10.9 and 11.7 °C in autumn, 5.7 and 7.1 °C in winter and 10.9 and 10.1 °C in spring during study cycles two and three, respectively. During the waterlogging treatment the mean temperature was 6.4 °C in the second and 7.5 °C in the third cycle (Kronberg et al., 2024).

Barley (*Hordeum vulgare*) was grown in all monoliths during the growing seasons while Tall Fescue (*Festuca arundinacea*) was under sown to half of the monoliths as an overwintering cover crop. Both barley and cover crop biomass were harvested and the dry mass was determined by drying at 105 °C for one hour and then overnight at 60 °C (Hakala et al., 2009). Afterwards, the cover crop was allowed to grow over the experimental winter and again harvested before the next cultivation. During each study cycle, all monoliths were fertilized equally using laboratory quality salts with applied nutrient levels corresponding to 90, 110 and 150 $kg\,N\,ha^{-1}$; 0, 12.5 and 25 $kg\,P\,ha^{-1}$; and 32, 25 and 100 $kg\,K\,ha^{-1}$ in cycles one, two and three, respectively. The fertilization was increased towards the end of the experiment to address nutrient deficiencies observed in barley. Micronutrients were applied

Table 1. Selected physical and chemical properties of the studied soils. The results accompanied by detailed analytical methods have been previously described in Kronberg et al. (2024).

	Depth	Soil C and N			pH_{H_2O}	Oxides		ρ_b	Particle size distribution		
	(cm)	Total C (%)	WEOC ($mg\,kg^{-1}$)	Total N (%)		Al_{ox} ($mmol\,kg^{-1}$)	Fe_{ox} ($mmol\,kg^{-1}$)	($kg\,dm^{-3}$)	Sand (%)	Silt (%)	Clay (%)
Silty clay	0–10	2.6	48	0.22	7.1	62	112	1.01	9	43	47
	10–20	2.3	50	0.20	7.0	69	117	1.11			
	20–30	1.2	41	0.10	7.0	57	77	1.50	6	34	60
	30–40	0.5	32	0.05	7.2	50	41	1.53			
	40–50	0.3	26	0.03	7.4	48	37	1.48	3	39	58
	50–60	0.3	24	0.02	7.5	35	35	1.43			
Sandy loam	0–10	1.7	33	0.15	6.6	109	51	1.13	67	16	17
	10–20	1.8	29	0.15	6.7	107	50	1.26			
	20–30	1.7	33	0.15	6.7	110	51	1.40	71	15	14
	30–40	1.4	39	0.10	6.8	155	50	1.39			
	40–50	0.7	47	0.03	6.8	171	50	1.31	84	11	5
	50–60	0.5	45	0.02	6.8	152	34	1.39			

Symbols and abbreviations: WEOC, water extractable organic carbon; Al_{ox}, Oxalate extractable aluminum (poorly ordered oxides); Fe_{ox}, Oxalate extractable iron (poorly ordered oxides); ρ_b, soil bulk density.

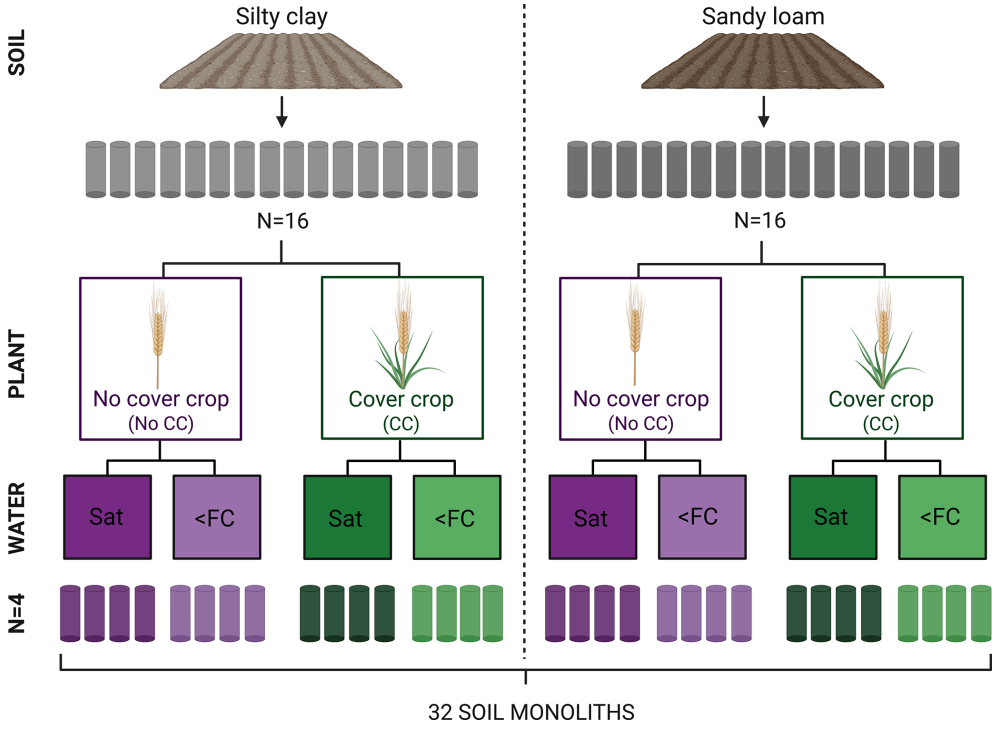

Figure 1. A schematic illustration of the soil monolith experiment study design. The 16 monoliths collected from each agricultural field (silty clay, sandy loam) were assigned to two levels of plant (No CC, No cover crop; CC, Cover crop) and water treatments (Sat, Water saturation; < FC, moisture maintained at 70 % field capacity).

as a foliar fertilizer (YaraVita Solatrel) during the second and third study cycles (Kronberg et al., 2024).

During the growing seasons all monoliths received equal irrigation of 17–27 mm per week via computer controlled Priva automated drip irrigation system (Greenhouse Environmental Control Systems, Priva BV, The Netherlands). Throughout the experiment, the monoliths were irrigated with artificial rainwater which was made according to the

ionic composition of typical rainwater in Southern Finland (Vet et al., 2014). After the harvest i.e., during the off-seasons, half of the monoliths received excessive manual irrigation until saturation was reached and water infiltration into the soil ceased (Saturation treatment). In the other half, the topsoil moisture was maintained at 70 % soil field capacity (< FC treatment) corresponding to ∼ 50 % water filled pore space (Kronberg et al., 2024). Soil moisture in all monoliths was adjusted according to soil moisture readings from Teros12 sensors. The waterlogging treatment was initiated by mimicking a 3 d heavy rainfall event (25 mm d^{-1}) that naturally occur in Southern Finland (Uusitalo et al., 2012; Virtanen et al., 2013). The drainage outlets were closed on the third day of the heavy rainfall event (taken as day 0 of waterlogging treatment). After, these monoliths were manually irrigated with 0–23 mm water per monolith per irrigation, and this was repeated several times per day if needed. Irrigation was stopped/paused once infiltration ceased. Whereas the silty clay soil got waterlogged already during the simulated heavy rainfall event, waterlogging of the sandy loam soil took on average 8 d longer due to the larger fraction of air-filled soil pores at the start of the excessive irrigation (Kronberg et al., 2024). In the second study cycle, some unfortunate leakages occurred in some sandy loam monoliths through sensor hole sealings, compromising complete waterlogging in the topsoil (further discussed in Kronberg et al., 2024). The length of the waterlogging treatment in cycles two and three was 54 and 50 d, respectively. The drainage was initiated by opening the drainage outlets.

2.2 CO_2 flux measurements

CO_2 fluxes were measured with a closed manual chamber system including an opaque cylindrical polypropylene chamber (d, 15.2 cm; h, 20–39 cm) and a non-dispersive infrared gas analyzer (Li 850, Li-cor Environmental, USA). The measurement system included a controlling unit with a tablet and a Raspberry Pi (Model 3B, Raspberry Pi Ltd., UK) computer running a custom-made Python program, enabling on-line monitoring of the gas mixing ratio development in the chamber headspace. The gas analyzers were installed in parallel in the sample line to prevent problems stemming from their pumps operating at different flow rates. The volume of the used chamber varied according to the plant height and ranged from 3.6–7.2 dm^3. The air inside the chamber was continuously mixed by a fan installed on the chamber sealing and the temperature was continuously monitored using a Pt-100-temperature probe and a Nokeval RMD 680 logger (Nokeval, Finland). The measurements were conducted weekly or bi-weekly during the off-seasons and bi-weekly during growing seasons.

On a measurement day each monolith was measured once for ∼ 7 min. The junction between the chamber and the monolith was sealed with plastic foil to make the chamber airtight. If any errors or leakages were observed during the closure, the measurement was repeated. The distance of the soil from the chamber edge was measured at least monthly. During the third study cycle, an empty chamber was measured before (and sometimes after) each measurement round to quantify any potential baseline fluxes. The median of the empty chamber flux for CO_2 was 1.25 mg m^{-2} h^{-1} (Q_1, 0.34; Q_3, 2.86; n, 25;). Accordingly, the empty chamber CO_2 flux was deducted from the measured CO_2 fluxes. Erroneous closures, identified by fluctuations in CO_2 mixing ratio, were excluded from further analysis

Gas fluxes were calculated by fitting a linear model to the gas mixing ratio data plotted against the closure time. The model fitting was conducted with a least squares method for the gas concentration change over 6 min. The first 30–45 s of the chamber closure were omitted to avoid errors caused by the system instabilities and pressure variations at closure (Pavelka et al., 2018). Linear fits of CO_2 mixing ratios against elapsed time were initially examined visually. Clear deviations from linearity were interpreted as evidence of leakage, typically caused by improper chamber insertion. Erroneous measurements were excluded by applying an R^2 threshold of 0.84. This threshold effectively removed all failed closures in cases where CO_2 flux exceeded three times the standard deviation of the flux measured in the empty chamber. For lower fluxes, R^2 values were generally below 0.84 even when the measurement was successful. These instances were therefore evaluated individually and excluded only when the CO_2 mixing ratio exhibited evident fluctuations indicative of leakage (0.4 % of the total data). The fluxes using the slope term dC/dt from the linear fit were calculated with the Eq. (1):

$$F = \frac{dC}{dt}\frac{M_{gas}\,p\,V}{R\,T\,A} \times 3600 \quad (1)$$

where F is the gas flux (g m^{-2} h^{-1}), M_{gas} molar mass of the gas (g mol^{-1}), p air pressure (101 325 Pa), V chamber volume (m^3), R ideal gas constant (8.314 J K^{-1} mol^{-1}), T air temperature (K) and A is a monolith surface area (m^2). Positive flux indicates an efflux of gas to the atmosphere.

As only dark chamber measurements were conducted, total ecosystem respiration, including CO_2 originating from both soil and plant components, was obtained. To estimate the fraction of CO_2 flux deriving specifically from the soil, aboveground cover crop biomass was removed 43 d after the initiation of waterlogging during the third study cycle. CO_2 fluxes were measured twice on the same day, immediately before and after biomass removal. The difference between the two measurements was assumed to represent respiration from aboveground plant tissues. This approach was applied to ensure that the observed differences between the cover crop and no cover crop treatments did not derive simply from the variation in aboveground biomass.

2.3 Dissolved C and Fe in soil porewater

Soil porewater samples were collected with Rhizon CSS samplers (pore size 0.15–0.2 µm, Rhizosphere Research Products B.V., The Netherlands) from three treatment replicates (monitored monoliths). At each sampling, needles (0.8×40 mm, Becton Dickinson, S.A., Spain) were inserted at the end of the samplers to connect them to 12 mL evacuated glass vials (Labco Limited, England) through rubber septa. Porewater samples were collected only from the monoliths belonging to the saturation treatment because suction was not adequate for sampling the monoliths maintained at 70 % FC. In the third cycle, samples were collected only during the waterlogging treatment, whereas in the second cycle, sampling was conducted both during the treatment and after the start of the drainage, with the final sampling done 16 d after. Total dissolved C (TDC), DOC and dissolved inorganic carbon (DIC) concentrations were measured with combustion catalytic oxidation method (TOC-L, Shimadzu Corporation, Japan) and total dissolved Fe concentration was measured colorimetrically with a 1,10-phenantroline method (Hill et al., 1978, see Kronberg et al., 2024). Samples were stored at −20 °C before the analysis.

2.4 Data analysis

Data analysis was conducted in R studio software environment with R version 4.4.3 (R Core Team, 2025). The impact of soil type as well as plant and water treatments on average CO_2 fluxes were tested with linear mixed effects model in glmmTMB package (Brooks et al., 2017). The effects were tested separately for the two study cycles. Monolith and measurement round were set as a random intercept to account for the repeated measurements and the non-independency of the data. The flux data was further divided into two temporal subgsroups, during and after the water treatment (but before the next cultivation), and the model was built separately for these time intervals due to their different flux dynamics. The models were first constructed with the likelihood method (ML), and the selection of interaction terms to include in the final models was done based on Akaike's information criteria (AIC) with stepAIC function and backwards method in MASS package (Venables and Ripley, 2002). Dropping interaction terms mostly improved the AIC apart from the period after waterlogging in cycle 3 for which the interaction between water and plant treatment was included. All main terms (soil type, water and plant treatments) were always included in the final model which was constructed with the restricted maximum likelihood method (REML). The assumptions of normality and homoscedasticity of the model error terms were inspected visually in all analyses. The significance level in all statistical analyses was set to 0.05.

To calculate cumulative CO_2 fluxes, we first generated daily flux values for each monolith by linearly interpolating between temporally consecutive measurement events using the na.approx function in the zoo package (Zeileis and Grothendieck, 2005). Next, the cumulative sum was calculated starting either from crop cultivation (beginning of the season) or from the beginning of the waterlogging treatment and calculated until next cultivation. The cumulative CO_2 fluxes calculated over the entire cycles were also further normalized for cumulative above ground biomass. The effect of soil, water and plant treatment on cumulative CO_2 fluxes was tested with linear model separately for the study cycles two and three. The assumptions of normality and homoscedasticity of the model residuals were visually evaluated by diagnostic plots. Biomass normalized cumulative CO_2 fluxes did not fulfill the assumption of residual normality and hence, Box–Cox transformation was applied (Box and Cox, 1964). Tukey' s post hoc tests were further applied to test the differences in between the treatments by using emmeans function in emmeans package (Russell, 2023). The comparison was done among the levels of water and plant treatments for each soil type and study cycle.

We also tested how well could a simple empirical model predict the CO_2 efflux during and after waterlogging events. CO_2 efflux was modelled in the monitored monoliths with an empirical equation utilizing an exponential temperature function (Kätterer et al., 1998) combined with a parabolic WFPS function (Luo and Zhou, 2006; Moyano et al., 2013) as follows:

$$F_{CO_2} = Q_{10}^{\frac{T-10}{10}} \times (-a \times \mathrm{WFPS}^2 + b \times \mathrm{WFPS}) \quad (2)$$

F_{CO_2} is the soil CO_2 efflux ($\mathrm{g\,m^{-2}\,d^{-1}}$), Q_{10} is the CO_2 temperature sensitivity factor, T is the measured soil temperature (°C) at 10 cm depth, WFPS is the water-filled pore space (%) calculated as the proportion of the measured SVWC at 10 cm from the maximum SVWC ($\mathrm{SVWC_{max}}$) in each monolith belonging to the saturation treatment. In the 70 % FC treatment, an average of the $\mathrm{SVWC_{max}}$ in the saturated monoliths in each soil type was used. In the equation, a, b and Q_{10} are parameters fitted for the two soils and two plant treatments separately. Residual standard error, adjusted R^2+ slope from the linear fit between the modelled and measured fluxes as well as the model residuals were used to evaluate the model performance. The constructed models were used to calculate the daily CO_2 flux for each monitored monolith with daily average values of soil T and WFPS ($n = 3$). Obtained fluxes were used to calculate the cumulative CO_2 fluxes similarly than with measured values starting from the beginning of the water treatment until next cultivation. The difference in cumulative fluxes calculated based on measured vs. modelled values was tested with pairwise t-test.

To study the relationship between dissolved C and Fe concentrations in soil porewater, repeated measures correlation analysis, where monolith was set as a participant/subject, was performed with rmcorr package (Bakdash and Marusich, 2024). Then, the concentrations of dissolved C species in soil pore water (c, $\mathrm{mgL^{-1}}$) were further converted to the

amount of C per liter soil ($mg\,L^{-1}$ soil). This was done to eliminate the apparent effect of SVWC on soil C contents in changing moisture conditions. In each monolith, the amount of accumulated DIC, i.e., the change in soil DIC storage (ΔDIC, $mg\,C\,m^{-2}$), during waterlogging was calculated with the Eq. (3).

$$\Delta\mathrm{DIC} = \frac{\sum_{\mathrm{Layer}=1}^{3} V \times (\theta_{\mathrm{end}} \times c_{\mathrm{end}} - \theta_{\mathrm{start}} \times c_{\mathrm{start}})_{\mathrm{Layer}}}{A} \quad (3)$$

In the equation, V, is the volume of each soil layer ($3.54\,dm^3$), A is the monolith surface area ($0.018\,m^2$), c_{end} and c_{start} are the soil porewater DIC concentrations ($mg\,L^{-1}$) at the end and at the first sampling of the waterlogging period, respectively, and θ_{end} and θ_{start} are the corresponding volumetric soil water contents. In cases where the c_{start} was not available for a specific soil monolith (no porewater obtained), the average of the first sampling round in each soil type and depth calculated based on available monoliths was used. The equilibrium porewater CO_2 concentration at the start was assumed to be similar within the same soil type and depth. The concentration was also assumed to be similar within each 20 cm soil layer around the sampling depth.

Characteristic of Finnish soils, neither of the studied soils contained significant amounts of carbonates (verified with 0.2 M HCl, "Fizz test") and thus, ΔDIC was assumed to consist mainly of dissolved CO_2 deriving from soil respiration. Thus, the total amount of respired CO_2 during the waterlogging was estimated by adding the ΔDIC to the cumulative CO_2 fluxes from each monolith. Only the waterlogging period from which porewater samples were collected was considered (Cycle 2: waterlogging days 0–49; cycle 3: days 7–45). In the 70 % FC treatment, only the cumulative CO_2 flux was considered because no porewater was obtained and the ΔDIC was assumed to be negligible because of the gas exchange with the atmosphere. The effect of time (days), soil type, plant treatment and depth on the concentration of TDC, DIC, DOC and total CO_2 production were tested with linear mixed effects model and nlme package (Pinheiro et al., 2023). A stepwise (backwards) model selection was performed with stepAIC function in MASS package (Venables and Ripley, 2002). The effect of waterlogging on total respired/produced CO_2 (in comparison to the 70 % FC treatment) was further tested by pairwise comparisons by emmeams function (Russell, 2023). The comparison was done separately for the two cycles within soil type and plant treatment.

3 Results

3.1 Measured CO_2 fluxes

During the waterlogging treatment the CO_2 fluxes were significantly ($p < 0.01$) lower in the saturated soil monoliths than in the control monoliths kept at 70 % FC (Fig. 2 and Table S1 in the Supplement). CO_2 fluxes from the saturated monoliths without cover crops were mostly around (cycle 2) or below (cycle 3) $0.5\,g\,C\,m^{-2}\,d^{-1}$, and fluxes in the monoliths with cover crop were significantly higher (+0.18 and $+0.87\,g\,C\,m^{-2}\,d^{-1}$ in cycles 2 and 3, respectively (Table S1). Upon drainage, the fluxes from the saturated monoliths increased to significantly higher level than in the 70 % FC treatment ($p < 0.001$, Fig. 2). The observed CO_2 pulse upon drainage was steeper in sandy loam compared to the silty clay soil (Fig. 2). After the CO_2 pulse, the differences between the two water treatments levelled out within two weeks in sandy loam soil. In silty clay soil, CO_2 fluxes from the previously saturated monoliths remained higher than from the non-saturated treatment until the next cultivation which was four weeks after drainage.

Waterlogging did not have a significant impact on off-season cumulative CO_2 fluxes in either of the study cycles, plant treatments or soils (Fig. 3). In the third cycle, however, the mean cumulative CO_2 fluxes in the saturated soils without the cover crop (silty clay $34 \pm 5.0\,g\,C\,m^{-2}$, sandy loam $40 \pm 4.9\,g\,C\,m^{-2}$) were slightly lower than in the 70 % FC treatment (silty clay $49 \pm 11.3\,g\,C\,m^{-2}$, sandy loam $46 \pm 7.0\,g\,C\,m^{-2}$). In turn, according to the linear model, the cover crop significantly increased the cumulative fluxes ($p < 0.01$), while the soil type did not have a significant impact on them ($p = 0.06$ or 0.87 in cycle two and three, respectively). The difference between the two plant treatments was larger in the third than in the second cycle (Fig. 3). According to the post hoc tests, the difference between the CC and No CC monoliths in the second cycle was not significant in either water treatment in sandy loam soil ($p = 0.08/0.09$) or in the 70 % FC treatment in silty clay ($p = 0.09$). The treatment-wise pattern in cumulative CO_2 fluxes over the entire study cycles (growing and off-seasons combined) remained consistent with those calculated for the off-seasons alone, but only when the fluxes were normalized for above-ground biomass (Fig. 3). Finally, cumulative CO_2 fluxes from the last off-season were also normalized per root biomass determined at the end of the experiment (see Kronberg et al., 2024 for details of root biomass determination). Once normalized per root biomass, cumulative CO_2 fluxes without cover crop were 3.7–6 times higher than with the cover crop (Fig. S2 in the Supplement).

In the 70 % FC treatment, the amount of above ground cover crop respiration, determined as the difference between the measured fluxes before and after above ground biomass removal, was on average $0.6 \pm 0.42\,g\,CO_2\,m^{-2}\,h^{-1}$ and $0.5 \pm 0.55\,g\,CO_2\,m^{-2}\,h^{-1}$ in silty clay and sandy loam monoliths, respectively. This represented 15 % and 12 % of the total CO_2 flux in silty clay and sandy loam, respectively. However, the averages were not statistically different from zero in either of the soils. Instead of a decrease, the above ground biomass removal induced an increase in CO_2 fluxes from saturated monoliths. In silty clay soil, the fluxes increased on average $0.6 \pm 0.88\,g\,m^{-2}\,d^{-1}$ while the increase in sandy loam soil

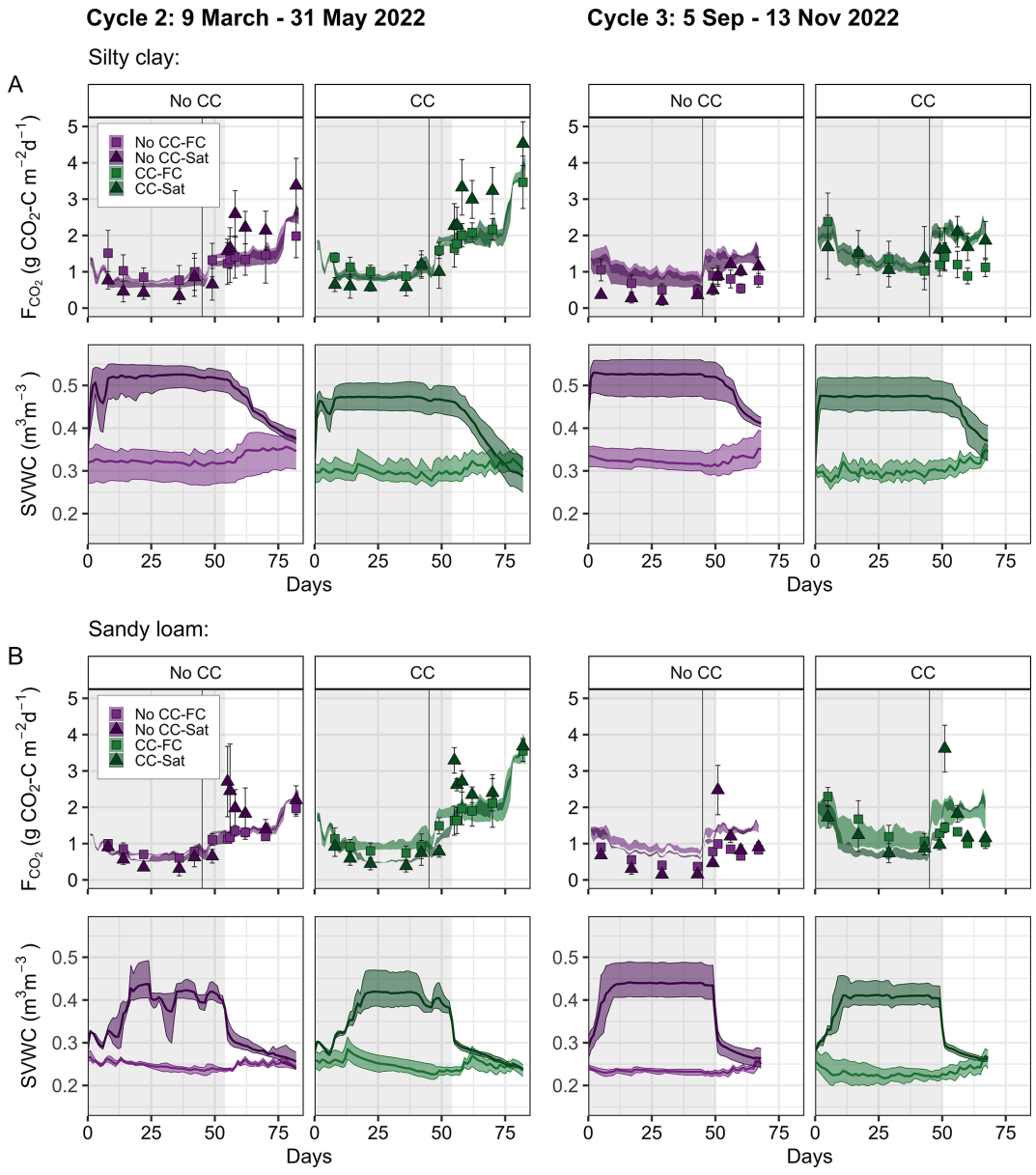

Figure 2. Measured (mean ± standard deviation, $n = 4$) and modelled (shaded ribbons, range, $n = 3$) CO_2 efflux and soil volumetric water content at 10 cm depth (SVWC, mean ± standard deviation, $n = 3$) during and after waterlogging in **(A)**. silty clay and **(B)** sandy loam soil during study cycles two and three CC, Cover crop; No CC, No cover crop; FC, 70 % field capacity; Sat, Water saturation). The gray shaded area represents the duration of the waterlogging event and the vertical solid line the day when the soil temperature was increased from 5–10° C for simulated spring. The x axis represents the number of days since the onset of the respective waterlogging event.

was modest, on average only $0.1 \pm 0.59\,\mathrm{mg\,m^{-2}\,d^{-1}}$. However, because of the large deviation between the replicate monoliths, the increases did not deviate from zero significantly.

3.2 CO_2 efflux modelled with the empirical model

Soil temperature dominated over moisture as the predictor for CO_2 efflux as indicated by the high Q_{10} and low a and b parameter values (Table 2). The modelled fluxes were very similar in the waterlogged and in 70 % FC treatment especially in silty clay soil (Fig. 2). The CO_2 flux dynamics and response to soil moisture were better captured (Fig. 2) and the model performance was overall better in sandy loam soil which is illustrated by the smaller RSE of the model and a larger R^2 of the linear model fitted for the predicted vs. measured data than in silty clay soil (Table 2). In both soils, model performed better with the cover crop than without the cover crop as indicated by higher R^2 (Table 2).

Table 2. Results of the temperature (T) and water filled pore space (WFPS) dependency model fit to CO_2 flux data from the monitored monoliths during the off-seasons. Also, the adjusted R^2, slope and intercept from the linear fit between the modelled and measured fluxes, used to evaluate model performance, are presented.

		$F_{CO_2} \sim T$, WFPS					Predicted ~ Measured		
		RSE	Q_{10}	a	b	n	Intercept	Slope	R^2
No cover crop	Silty clay	2.24	3.49	0.0009	0.13	145	2.73	0.38	0.39
	Sandy loam	1.88	3.31	0.0010	0.13	150	2.42	0.41	0.45
Cover crop	Silty clay	2.22	4.79	0.0008	0.14	150	2.58	0.60	0.59
	Sandy loam	1.93	3.79	0.0018	0.21	150	2.14	0.65	0.66

RSE = Residual standard error of the model ($g C m^{-2} d^{-1}$), Q_{10} = fitted CO_2 flux temperature sensitivity parameter, a and b = fitted model parameters, n = number of observations, Intercept = intercept of the linear regression fitted for modelled and measured CO_2 fluxes, Slope = slope of the linear regression, R^2 = adjusted coefficient of determination of the linear regression.

Towards the end of the waterlogging, the model overestimated the fluxes in the saturation treatment. In turn, the model could not reproduce the CO_2 peak measured after the initiation of drainage which led to underestimation of the fluxes (positive residuals) upon drainage in the monoliths belonging to the saturation treatment (Figs. 2 and S1 in the Supplement). During the third waterlogging, the model overestimated the CO_2 fluxes in the monoliths without the cover crop (Fig. 2). In cycle two, the cumulative CO_2 efflux calculated with modelled data was in good agreement with those calculated from the measured data with no statistically significant difference between the two (Fig. 3 and Table S3 in the Supplement). During cycle three, the same was true only for the monoliths with the cover crop. Without cover crops, cumulative CO_2 efflux obtained from the modelled CO_2 fluxes was significantly higher in both soils and water treatments (Fig. 3 and Table S3).

3.3 Dissolved C dynamics in porewater

TDC content increased during waterlogging at 10 and 30 cm depths in both soils and under both plant treatments (Fig. 4). The observed increase was attributed to the increased DIC content while DOC content remained relatively unchanged. The increases in TDC and DIC contents during waterlogging at 30 cm depth were more pronounced in sandy loam than in silty clay, whereas especially in the second cycle the increase in DIC content in the top 10 cm layer was steeper in silty clay. In sandy loam, waterlogging induced an increase in DIC content also at 50 cm depth (Fig. 4).

At 10 cm depth the contents of all dissolved C species (TDC, DIC, DOC) were significantly higher in silty clay than in sandy loam soil as illustrated by the significant soil term (for TDC, DIC, DOC) as well as the significant interaction of soil and waterlogging days (for TDC, DIC) in the mixed effects models (Table S4–S6 in the Supplement). Cover crops increased the TDC content in the silty clay topsoil while in sandy loam the increase was more pronounced at 30 cm depth (Fig. 4). In the third cycle, the average DOC content at 50 cm depth was significantly higher in the monoliths with the cover crop than without in sandy loam soil ($p = 0.01$) (Fig. S2), while there was no statistically significant difference during the second cycle (Table S6).

During the second off-season, porewater TDC concentration correlated with dissolved Fe concentration at 10 and 30 depths in silty clay soil both with (10 cm: $r = 0.51$, $p = 0.023$; 30 cm: $r = 0.58$, $p = 0.005$) and without the cover crop (10 cm: $r = 0.46$, $p = 0.049$; 30 cm: $r = 0.58$, $p = 0.006$), and in sandy loam with the cover crop (10 cm: $r = 0.58$, $p = 0.009$; 30 cm : $r = 0.59$, $p = 0.07$) (Table S9 in the Supplement). In silty clay soil, the correlation with dissolved concentration was attributed to the changes in DIC concentration in both plant treatments (Fig. 5a), whereas in sandy loam Fe concentration correlated with DOC instead, however, only in the topsoil (Fig. 5d). During the third cycle the porewater C and Fe concentrations were only measured during the waterlogging (excluding the drainage phase) and then, the DOC concentration did not exhibit positive correlation with Fe in either soil at any depth (Table S9). During this cycle, the correlation between DIC and Fe concentrations, in turn, was significant in both soils with the cover crop at 30 cm (silty clay: $r = 0.88$, $p < 0.001$; sandy loam: $r = 0.71$, $p = 0.022$) and in silty clay at 10 cm with the cover crop ($r = 0.75$, $p = 0.013$) (Table S9).

3.4 Total CO_2 production as the sum of cumulative CO_2 fluxes and ΔDIC

Results from the linear model showed that waterlogging decreased the total CO_2 production (cumulative CO_2 flux + ΔDIC) statistically significantly during the second ($p = 0.002$) but not during the third ($p = 0.10$) waterlogging (Fig. 6 and Table S7 in the Supplement). However, according to the pairwise comparisons, the means of the two water treatments within each soil type and plant treatment were only statistically significantly different in silty clay soil in cycle two without the cover crop (Fig. 6 and Table S8 in the Supplement). In the third cycle CO_2 production was statistically significantly higher with the cover crop than without ($+35 g C m^{-2}$, $p < 0.01$) while there was no difference in

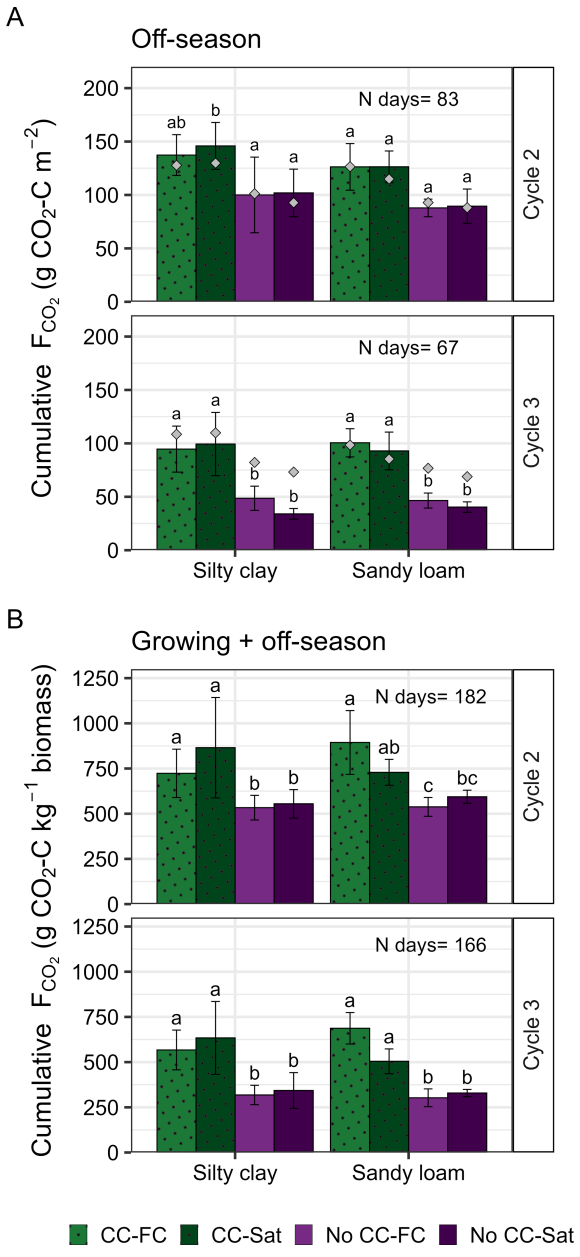

Figure 3. Cumulative CO_2 fluxes (as $g CO_2 - C$) calculated for the off-season starting from the initiation of the waterlogging treatment until the next cultivation (Cycle 2) or until the end of the experiment (Cycle 3) **(A)**, and for the entire study cycle (Cycle 2, Cycle 3) normalized to the cumulative above ground biomass (kg^{-1} aboveground biomass) **(B)**. Mean ± standard deviation ($n = 4$) of the replicated monoliths (CC-FC, Cover crop and 70 % field capacity; CC-Sat, Cover crop and Water saturation; No CC-FC, No cover crop and 70 % field capacity; No CC-Sat, No cover crop and Water saturation). Gray squares illustrate the mean ($n = 3$) cumulative flux from the empirical temperature and moisture dependency model. *N days* represents the number of days included in the calculation of the cumulative sums, and lower-case letters the statistical differences within each soil type and cycle.

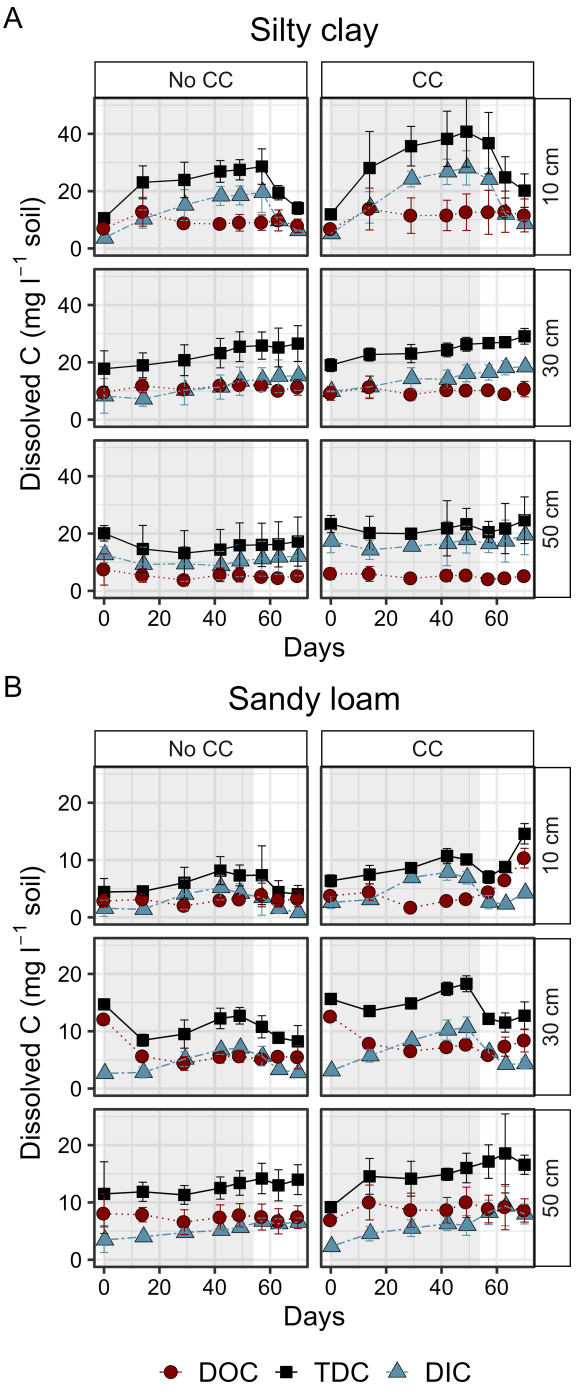

Figure 4. Timeseries of dissolved organic carbon (DOC), inorganic carbon (DIC) and total dissolved carbon (TDC) contents as $mg C L^{-1}$ soil (mean ± standard deviation, $n = 3$) during (shaded area) and after waterlogging in silty clay **(A)** and sandy loam **(B)** soil profiles with and without cover crops (No CC, No cover crops; CC = Cover crops) in cycle two. Days on the x axis represent the days since the beginning of waterlogging. Note the differing scales on y axis in the two soils. Data from cycle three is presented in Fig. S1.

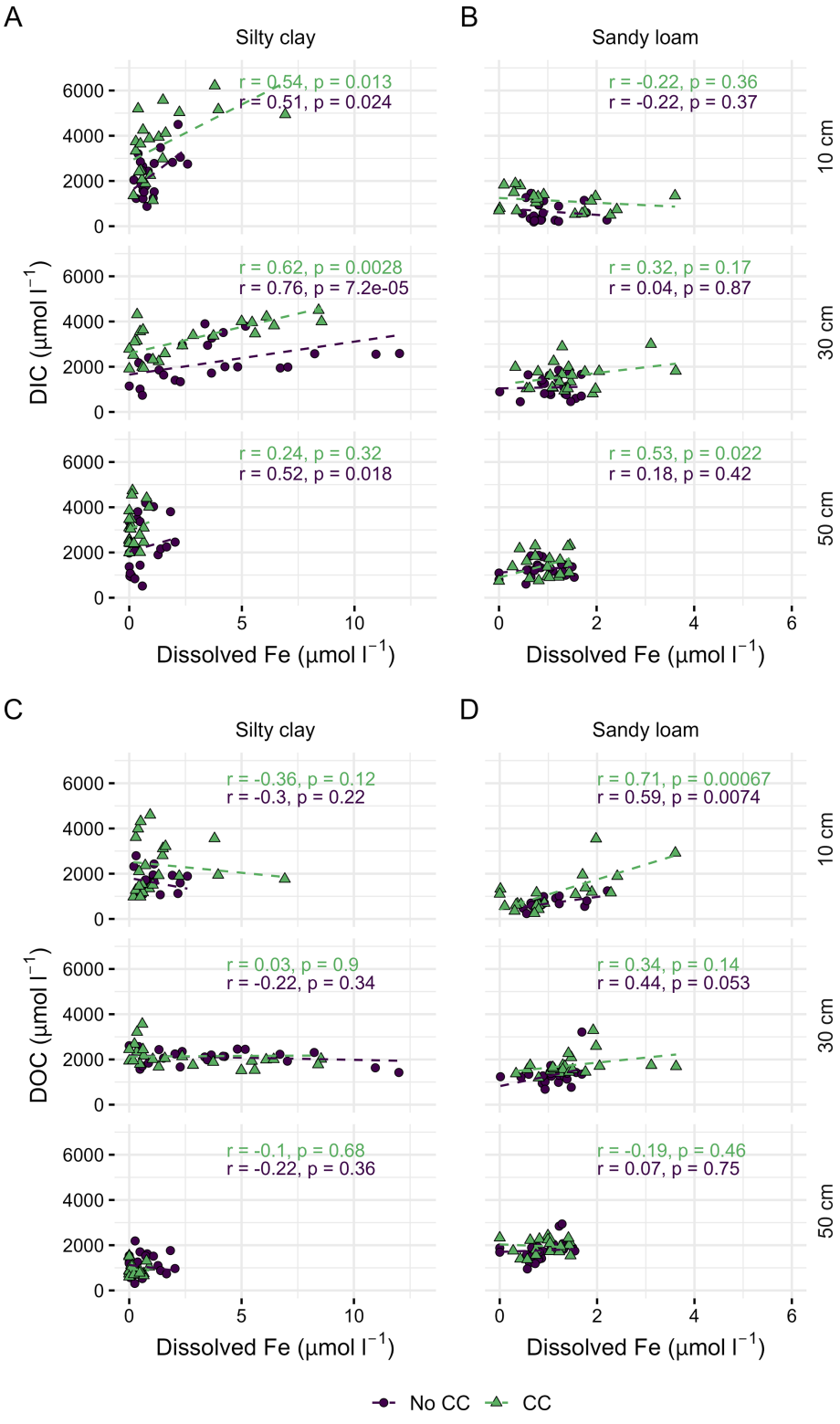

Figure 5. Relationship between porewater dissolved Fe and dissolved inorganic carbon (DIC) **(A, B)** and dissolved organic carbon (DOC) **(C, D)** in the soils belonging to the saturation treatment, and with (CC) and without the cover crop (No CC) at different depths. The regression lines, and the correlation coefficients (r) together with the corresponding p values were obtained from repeated measures correlation analysis. Observe the differing x axis scales in the two soils.

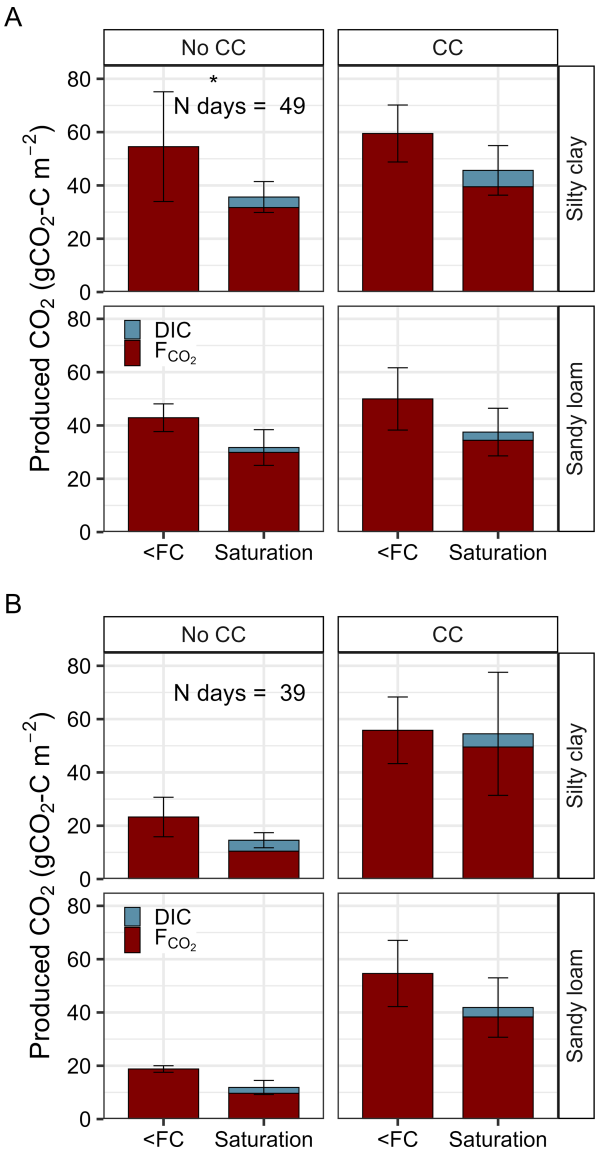

Figure 6. Total produced CO_2-C as the sum of cumulative CO_2 flux and accumulated DIC in soil pore water during the second **(A)** and third **(B)** waterlogging in silty clay and sandy loam soil with (CC) and without (No CC) cover crops. Statistically significant differences between the two water treatments are marked with asterisks.

the second cycle ($p = 0.1$). Soil type was significant in cycle two where the total CO_2 production during waterlogging was lower in sandy loam than in silty clay ($-8.3\,g\,C\,m^{-2}$, $p = 0.05$) (Fig. 6). Soil type was not significant in cycle three.

The amount of the accumulated DIC in the saturated monoliths corresponded to on average 6 %–29 % of the total CO_2 production during waterlogging. In the second cycle, the percentage was on average 11.5 ± 5.7 % (No CC) and 13.5 ± 0.4 % (CC) in silty clay, and 6.0 ± 1.7 % (No CC) and 8.8 ± 3.9 % (CC) in sandy loam. In the third cycle, the percentage was larger in No CC treatment (silty clay 28.8 ± 2.5 %, sandy loam 19.8 ± 2.6 %) but it remained at a similar level in the CC treatment (silty clay 9.4 ± 1.4 %, sandy loam 8.9 ± 2.4 %).

4 Discussion

4.1 Impact of waterlogging on measured CO_2 fluxes

We studied the impact of periodic off-season waterlogging on soil C dissolution, and CO_2 emissions in a controlled mesocosm study with intact soil profiles with and without Tall Fescue as a cover crop. In our experiment, temporary soil waterlogging lasting ~ 50 d at an average soil temperature of ~ 7 °C did not significantly alter cumulative CO_2 emissions calculated over waterlogging and the subsequent drainage period. Our results align with findings from several incubation studies suggesting that temporary anaerobic conditions may exert only a minor impact on C decomposition and cumulative greenhouse gas emissions (e.g. Bhattacharyya et al., 2018; Hanke et al., 2013; Huang et al., 2021; Tete et al., 2015; Winkler et al., 2019). However, previous studies have reported effects in both directions, depending on soil characteristics, and the nature and duration of redox conditions.

While static anoxic conditions have suppressed C losses in several studies (Fairbairn et al., 2023; Huang et al., 2020; Tete et al., 2015), as traditionally believed, oxic-anoxic fluctuations have led to equal or greater C losses (Huang et al., 2021; Jeanneau et al., 2020; Tete et al., 2015). In the laboratory incubations by Huang et al. (2021) and Tete et al. (2015), reduced decomposition during anaerobic period(s) was compensated by increased CO_2 efflux during the following aerobic period(s) in weekly to monthly timescale. This pattern is consistent with our results: the cumulative CO_2 fluxes remained unaffected by waterlogging but the temporal flux dynamics differed between the two water treatments. The reduced CO_2 fluxes during waterlogging were compensated for by the higher fluxes after the drainage in both soils. Based on these observations, during transient anaerobic events, most CO_2 fluxes tend to occur during the subsequent drainage/aerobic phase which makes the calculation of cumulative emissions sensitive to the chosen observation period. Thus, our results underscore the importance of considering the following drying period in assessing the impacts of waterlogging on soil CO_2 efflux under fluctuating moisture conditions.

According to Ginn et al. (2017), repeated anoxic-oxic cycles increase soil Fe reducibility, which may, in turn, enhance C availability and promote C mineralization. Among the soils used in our experiment, the silty clay soil had experienced fluctuating redox conditions in field as indicated by its stagnic properties. It also contained a higher Fe oxide content than the sandy loam. Therefore, we expected that waterlogging would enhance C availability and mineralization more

strongly in silty clay soil. Yet, contrary to our hypothesis, the cumulative CO_2 fluxes (calculated over the waterlogging and the following drainage period), and their response to waterlogging, were similar in the two soils. Only a slight difference between the two soils was observed in CO_2 production during waterlogging in the second study cycle. This lack of clear differences between the two soils contradicts with the higher DOC and DIC contents measured in the silty clay than in the sandy loam topsoil during waterlogging, implying a higher mineralization rate in the silty clay during both study cycles. The dissolved C dynamics in deeper soil layers, however, help to explain the lack of difference in the aggregated CO_2 fluxes from the whole profile.

In sandy loam the increase in DIC was more modest in the topsoil than in silty clay but the content increased more evenly at all soil depths. This suggests that while CO_2 production was lower in the sandy loam topsoil compared to silty clay, higher microbial activity at deeper depths increased the total respiration per area, thereby narrowing the difference in cumulative CO_2 emissions between the two soils. Most studies on soil C dynamics focus exclusively on changes in the top 0–20 cm soil layer (Poeplau and Don, 2015). However, it has been demonstrated that examining the entire soil profile can yield conclusions that greatly differ from those based solely on topsoil analysis (Tautges et al., 2019). Thus, our findings emphasize that C dynamics in deeper soil layers may play a significant role in overall C dynamics and should therefore not be overlooked in future studies.

4.2 Belowground C dynamics during waterlogging

4.2.1 Waterlogging causes a discrepancy between respired CO_2 and

Increasing soil DIC concentrations – reflecting the accumulation of CO_2 within soil pores – indicated that during waterlogging, C mineralization continued at a higher rate than would have been inferred from CO_2 flux measurements alone. In our experiment, accumulated CO_2 (ΔDIC) was at most $\sim 30\,\%$ of the total CO_2 production during waterlogging (sum of cumulative CO_2 fluxes and ΔDIC) which is in a good agreement with previously reported values (Maier et al., 2011; Sánchez-Cañete et al., 2018). The accumulation of CO_2 results from impeded diffusive gas transport under waterlogged conditions (Greenway et al., 2006), causing CO_2 to be retained in the soil and released upon re-drying, when a peak in CO_2 efflux was observed. Consequently, the discrepancy between CO_2 production and measured efflux demonstrates that momentary soil CO_2 efflux should not be considered equivalent to soil respiration as the two are decoupled in transiently high soil moisture events (Maier et al., 2011; Ryan and Law, 2005; Sánchez-Cañete et al., 2018). Thus, the immediate response of CO_2 efflux to soil waterlogging reflects not only the moisture sensitivity of heterotrophic respiration but also the concurrent constraints on gas transport.

The discrepancy between CO_2 production and efflux likely caused the empirical CO_2 efflux model to fail in simulating the flux dynamics and capturing the post-drainage CO_2 pulse. The model was unable to reproduce the CO_2 pulse upon drainage because the pulse did not represent momentary soil respiration but was largely a consequence of the release of previously respired CO_2. These results support previous evidence that simple models may underestimate the CO_2 production during water saturated, anaerobic conditions (e.g. Fairbairn et al., 2023).

To account for the difference in measured CO_2 efflux and soil respiration, Maier et al. (2011, 2010) and Hirsch et al. (2004) have proposed an incorporation of a storage flux term in soil moisture dependency models. They defined the storage flux as the flux resulting from changes in the amount of CO_2 stored in soil (Hirsch et al., 2004; Maier et al., 2011, 2010). We believe that incorporating a storage flux term could have also improved model performance in our study. However, a robust implementation would have required higher spatial resolution of DIC measurements across the soil profile. Overall, to accurately model C dynamics during transient or temporary waterlogging, process-based approaches that account for anaerobic CO_2 production (Fairbairn et al., 2023) and changes in gas transport should be considered.

4.2.2 Processes contributing to the increase in dissolved C content

We hypothesized that soil waterlogging would promote mobilization of the Fe associated C and therefore result in an increase in soil DOC content, as commonly observed in incubation studies (e.g. Chen et al., 2020; Huang and Hall, 2017; Pan et al., 2016; Winkler et al., 2019). As opposed to our hypothesis, soil DOC content did not increase in either soil during waterlogging; the only clear increase was observed in sandy loam topsoil after drainage, likely due to enhanced OM decomposition and plant root exudation. However, TDC content increased during waterlogging, suggesting that an immediate microbial mineralization of DOC to CO_2 may have masked any increases in DOC content, with the effect instead becoming apparent as an increase in DIC (Fairbairn et al., 2023). In addition to mobilization of mineral associated C, in the presence of plant cover, the accumulating CO_2 (DIC) may have also originated from root respiration or from the decay of root litter (Kuzyakov, 2006). The above-mentioned processes and their contributions to increased TDC/DIC are discussed next.

Our results suggest that the contribution of Fe dissolution and the mobilization of associated C in the overall increase in TDC/DIC content was likely small. Waterlogging appeared to induce only slight reductive Fe dissolution since the Fe concentrations in porewater remained low throughout

the study (max $\sim 10\,\mu mol\,L^{-1}$) (Kronberg et al., 2024). In silty clay topsoil, for instance, the highest average DIC concentration during the second cycle ($\sim 3\,mmol\,L^{-1}$) was three orders of magnitude higher than that of Fe ($\sim 2\,\mu mol\,L^{-1}$). Thus, although soil DIC concentration correlated with Fe concentration during waterlogging, particularly in silty clay soil, the dissolution of Fe-OC alone can not explain the observed increases in DIC/TDC. Vice versa, the higher dissolved C content, reflecting soil microbial/rhizospheric activity, may have rather enhanced Fe dissolution slightly, as also seen in previous studies (e.g. Winkler et al., 2019). Overall, substrate availability was likely not substantially enhanced by waterlogging, as cumulative CO_2 fluxes did not increase relative to the 70 % FC treatment.

Root respiration, including the activity of roots and closely associated microbes, can represent between 10 % and 90 % of the total soil respiration (Hanson et al., 2000). In our experiment DIC increased only slightly more with the cover crop than without despite the ~ 10 times higher root biomass at 0–20 cm depth with the cover crop (Kronberg et al., 2024). Thus, if a substantial fraction of the accumulated DIC in soil would have derived from root respiration, we would have expected a larger difference in the produced DIC. In fact, during waterlogging, cover crops had a more pronounced effect on measured CO_2 fluxes than on DIC, and thus, we think that a significant fraction of the CO_2 respired by cover crop roots was released to the atmosphere directly through their stems. Indeed, it has previously been demonstrated that a substantial amount root-derived CO_2 can be transported to the atmosphere via transpiration stream in plant xylem (Aubrey and Teskey, 2021, 2009). Although this mechanism could not be verified with our experimental setup, the transport of CO_2 through Tall Fescue stems seems highly likely, as the species has been shown to develop aerenchyma under waterlogged conditions, enhancing gas exchange between the rhizosphere and the atmosphere (Mui et al., 2021). This feature is specific to Tall Fescue and has not been shown to apply to many other commonly used cover crop species, such as annual ryegrass for example.

If the dissolution of Fe-associated C and root respiration can account only for small portions of the observed increases in TDC, what are the remaining potential sources? In addition to direct release of C from Fe associations, the commonly observed increase in C solubility upon flooding has been attributed to pH-driven OC desorption from mineral phases (Grybos et al., 2009; Pan et al., 2016), dispersion of soil colloids (Buettner et al., 2014) and accumulation of microbial metabolites and fermentation products in anaerobic conditions (Fairbairn et al., 2023; Tete et al., 2015). The circumneutral initial pH of the soils in our experiment resulted in a slight decrease rather than an increase in pH during waterlogging which was likely caused by an accumulation of CO_2 as carbonic acid and bicarbonate (H_2CO_3, HCO_3^-) (Kronberg et al., 2024). Thus, desorption driven by the pH increase (Grybos et al., 2009) was unlikely. In soil, fermentation and Fe reduction are often coupled (Lovley, 1991; Snoeyenbos-West et al., 2000). Had fermentation proceeded at a much higher rate than Fe reduction in our system, we would have expected a more pronounced initial accumulation of organic metabolites and fermentation products, reflected as an increase in DOC content.

Finally, we want to bring up the possibility that O_2 entrapped in soil pores upon water saturation could have formed aerobic microenvironments (Williams and Oostrom, 2000) where aerobic respiration could go-on and contribute to an increased soil DIC and TDC content. Huang and Hall (2017) speculated that anoxic-oxic interfaces may play an important role in the observed increases in C mineralization during waterlogging periods. The porous and heterogenous soil matrix often leads to significant spatiotemporal variability in soil redox conditions as well as microbial metabolic rates and pathways (Fiedler, 2000; Keiluweit et al., 2017). Thus, despite the low redox potentials measured in our study (Kronberg et al., 2024), aerobic microsites may have facilitated aerobic instead of anaerobic respiration, thereby contributing to CO_2 production during waterlogging.

4.3 Impact of the cover crop on C mineralization

We expected that Tall Fescue as a cover crop would alter the response of soil CO_2 production to waterlogging because of increased substrate availability promoting C mobilization. As opposed to our hypothesis, the response of cumulative CO_2 fluxes to waterlogging was similar in both plant treatments. This suggests that cover crop root C inputs did not significantly promote mobilization of OM from mineral phases as reported by e.g. Winkler et al. (2019), although higher dissolved C content in the cover crop treatment appeared to slightly enhance Fe solubility. Despite careful soil moisture monitoring, slight oscillations in soil moisture occurred due to cover crop transpiration in the sandy loam topsoil. This introduced a minor confounding effect on soil redox state, as noted in our preceding study (Kronberg et al., 2024). While we consider the impact on C fluxes to be small, it may have facilitated more efficient gas transport from soil to the atmosphere. Furthermore, the specific feature of Tall Fescue being able to form aerenchyma, which facilitates O_2 transport into the roots, may have mitigated its effects on Fe-associated C by accelerating the drop in soil redox potential less than anticipated (Kronberg et al., 2024). Therefore, these findings should not be generalized to other cover crop species.

The applied methodology does not allow us to distinguish soil respiration from total ecosystem respiration which unfortunately prevents a direct assessment of waterlogging effects on soil versus plant respiration. However, measurements taken during the third waterlogging event, following the removal of aboveground cover crop biomass, showed that cover crop respiration was relatively low ($0.6\,g\,C\,m^{-2}\,d^{-1}$) compared to the average difference in CO_2 fluxes between monoliths with and without the cover crop ($3.2\,g\,C\,m^{-2}\,d^{-1}$).

This indicates that the overall higher CO_2 emissions from the monoliths with the cover were likely driven by belowground processes rather than by aboveground autotrophic respiration. Furthermore, higher cumulative CO_2 emissions with the cover crop persisted when normalized to cumulative above ground biomass further suggesting that the higher fluxes were not resulting from above ground autotrophic respiration. In fact, cover crop biomass was minor compared to barley biomass ($\sim 12\,\%$, data not shown) while the root biomass was significantly larger under the cover crop treatment as presented in our previous publication (Kronberg et al., 2024).

Normalizing cumulative CO_2 fluxes from the last off-season to root biomass in the top 20 cm of soil showed that the fluxes per gram of root biomass were approximately three times higher without cover crops than with them (Fig. 3). This suggests that although the cover crop increased the CO_2 emissions per m^2, the plant cover had a net positive effect on soil C sequestration because emissions per soil C input (i.e. root biomass) were smaller. Thus, potential priming effects of the cover crop on OM (not directly measured) did not appear to be substantial enough to offset the positive contributions of the cover crop to soil C storage. Hence, our results tentatively suggest that cover crops had a net positive effect on soil C sequestration, even under periodic waterlogging, which is in line with studies that have promoted cover crops as effective strategy to improve soil C sequestration (Heikkinen et al., 2022; Kaye and Quemada, 2017; Poeplau et al., 2015; Poeplau and Don, 2015).

4.4 Environmental implications and research outlook

A recent study showed that many agricultural fields in Finland already experience periodic waterlogging during late autumn when transpiration is low and rainfall is high (Mattila and Vihanto, 2024). This highlights the urgent need to apply mechanistic insights on the effects of temporary waterlogging on C dynamics from laboratory incubations to field scale, with our mesocosm study acting as a crucial bridge between the two. Our results suggest that waterlogging outside growing seasons might not significantly affect net C mineralization in cultivated mineral soils in a cool, humid climate. Accordingly, the associated risk of soil C loss and resulting climate feedbacks may be smaller than anticipated from laboratory incubation studies, which have largely focused on tropical and volcanic soils (e.g. Bhattacharyya et al., 2018; Huang et al., 2020; Winkler et al., 2019). However, our study focused merely on the effects of altered soil moisture on CO_2 fluxes and dissolved C dynamics, without accounting for potential impacts on C inputs, soil N dynamics or on production of another potent greenhouse gas, nitrous oxide (N_2O). It is also important to recognize that besides soil moisture, climate change-induced shifts in e.g. off-season soil temperatures and freeze–thaw cycles are likely to affect greenhouse gas emissions and soil C sequestration capacity (Heikkinen et al., 2022; Liu et al., 2024). Thus, studies that evaluate the net impacts from these factors in an integrated manner are warranted in the future.

From the methodological perspective, we want to highlight that the changes in soil CO_2 storage during and after high soil moisture events should not be overlooked as neglecting these changes could lead to biased view of momentary soil respiration. In modelling, model-data synthesis is used to match modelled results with the measured fluxes facilitating the calibration of C cycling simulation models (Nevalainen et al., 2022) and enabling the assessment of individual climate parameters' effects on the outcome (Heimsch et al., 2024). The lag between respiration and the release of the respired CO_2 to the atmosphere will make such model-data synthesis challenging, as the measured CO_2 efflux may result from respiration over the preceding weeks. Incorporating the temporary storage of dissolved CO_2 into models would improve the accuracy of the simulation of short-term dynamics and ensure that the respiration terms would be fitted based on the correct time period under when they occur.

We conclude that because surface CO_2 fluxes reflect the net soil–atmosphere release, which depends not only on production but also on transport and temporary storage within the soil profile, simple empirical models are unable to capture momentary soil respiration. Moreover, the continued CO_2 production observed under anaerobic, water-saturated conditions supports previous findings that temporary waterlogging does not suppress CO_2 production in mineral soils to near zero. Despite the important role of short-range-ordered Fe-oxides in C stabilization in boreal agricultural soils, the dissolution and mobilization of associated C did not appear to be the primary driver of the sustained CO_2 production. Furthermore, root C inputs from Tall Fescue, used as an overwintering cover crop, did not promote a substantial release of Fe-associated C, as indicated by low dissolved Fe concentrations and an unaltered soil CO_2 efflux response to waterlogging in the presence of plant cover. Overall, our results suggest that off-season waterlogging in a cool, humid climate has no effect on total CO_2 emissions from cultivated mineral soils.

Data availability. The data have been published in Zenodo (https://doi.org/10.5281/zenodo.14438980; Kronberg et al., 2025).

Supplement. The supplement related to this article is available online at https://doi.org/10.5194/bg-23-2431-2026-supplement.

Author contributions. RK: Conceptualization, Formal analysis, Funding acquisition, Investigation, Methodology, Project administration, Visualization, Writing – original draft, Writing – review and editing. SK: Conceptualization, Methodology, Supervision, Writing – review and editing. MP: Conceptualization, Methodology, Su-

pervision, Funding acquisition, Project administration, Writing – review and editing. TP: Methodology, Software. MK: Methodology, Software, Writing – review and editing. TM: Supervision, Writing – review and editing.

Competing interests. The contact author has declared that none of the authors has any competing interests.

Disclaimer. Publisher's note: Copernicus Publications remains neutral with regard to jurisdictional claims made in the text, published maps, institutional affiliations, or any other geographical representation in this paper. The authors bear the ultimate responsibility for providing appropriate place names. Views expressed in the text are those of the authors and do not necessarily reflect the views of the publisher.

Acknowledgements. R.K. acknowledges the University of Helsinki Doctoral Programme in Sustainable Use of Renewable Natural Resources (AGFOREE) for financial support as a doctoral scholarship. We are grateful for Jussi Heinonsalo (University of Helsinki) for his valuable contributions to the experimental conceptualization and planning. We also want to thank Rauna Lilja and Lisa Leinonen for their contributions to establishing and maintaining the experiment. Figure 1 was created in BioRender (Kronberg, 2025).

Financial support. This research has been supported by the Research Council of Finland (grant-nos. 337549, 328309, and 327236), the Research Council of Finland (grant-no. 339489), the Maa-ja Vesitekniikan Tuki Ry (grant-no. 44875), and the Salaojituksen Tukisäätiö sr (grant-no. H-13-2022-9.1).

Open-access funding was provided by the Helsinki University Library.

Review statement. This paper was edited by Sara Vicca and reviewed by two anonymous referees.

References

Asano, M., Wagai, R., Yamaguchi, N., Takeichi, Y., Maeda, M., Suga, H., and Takahashi, Y.: In Search of a Binding Agent: Nano-Scale Evidence of Preferential Carbon Associations with Poorly-Crystalline Mineral Phases in Physically-Stable, Clay-Sized Aggregates, Soil Syst., 2, 32, https://doi.org/10.3390/soilsystems2020032, 2018.

Aubrey, D. P. and Teskey, R. O.: Root-derived CO_2 efflux via xylem stream rivals soil CO_2 efflux, New Phytol. 184, 35–40, https://doi.org/10.1111/j.1469-8137.2009.02971.x, 2009.

Aubrey, D. P. and Teskey, R. O.: Xylem transport of root-derived CO_2 caused a substantial underestimation of belowground respiration during a growing season, Glob. Change Biol., 27, 2991–3000, https://doi.org/10.1111/gcb.15624, 2021.

Bakdash, J. Z. and Marusich, L. R.: rmcorr: Repeated Measures Correlation, https://CRAN.R-project.org/package=rmcorr (last access: 8 April 2026), 2024.

Bhattacharyya, A., Campbell, A. N., Tfaily, M. M., Lin, Y., Kukkadapu, R. K., Silver, W. L., Nico, P. S., and Pett-Ridge, J.: Redox Fluctuations Control the Coupled Cycling of Iron and Carbon in Tropical Forest Soils, Environ. Sci. Technol., 52, 14129–14139, https://doi.org/10.1021/acs.est.8b03408, 2018.

Bingeman, C. W., Varner, J. E., and Martin, W. P.: The Effect of the Addition of Organic Materials on the Decomposition of an Organic Soil. Soil Sci. Soc. Am. J., 17, 34–38, https://doi.org/10.2136/sssaj1953.03615995001700010008x, 1953.

Box, G. E. P. and Cox, D. R.: An Analysis of Transformations, J. R. Stat. Soc. B, 26, 211–243, https://doi.org/10.1111/j.2517-6161.1964.tb00553.x, 1964.

Brooks, M. E., Kristensen, K., van Benthem, K. J., Magnusson, A., Berg, C. W., Nielsen, A., Skaug, H. J., Machler, M., and Bolker, B. M.: glmmTMB balances speed and flexibility among packages for zero-inflated generalized linear mixed modelling, The R journal, 9, 378–400, https://doi.org/10.3929/ethz-b-000240890, 2017.

Buettner, S. W., Kramer, M. G., Chadwick, O. A., and Thompson, A.: Mobilization of colloidal carbon during iron reduction in basaltic soils, Geoderma, 221–222, 139–145, https://doi.org/10.1016/j.geoderma.2014.01.012, 2014.

Chandregowda, M. H., Tjoelker, M. G., Pendall, E., Zhang, H., Churchill, A. C., and Power, S. A.: Belowground carbon allocation, root trait plasticity, and productivity during drought and warming in a pasture grass, J. Exp. Bot, 74, 2127–2145, https://doi.org/10.1093/jxb/erad021, 2023.

Chen, C., Hall, S. J., Coward, E., and Thompson, A.: Iron-mediated organic matter decomposition in humid soils can counteract protection, Nat. Commun., 11, 2255, https://doi.org/10.1038/s41467-020-16071-5, 2020.

Clemmensen, K. E., Bahr, A., Ovaskainen, O., Dahlberg, A., Ekblad, A., Wallander, H., Stenlid, J., Finlay, R. D., Wardle, D. A., and Lindahl, B. D.: Roots and Associated Fungi Drive Long-Term Carbon Sequestration in Boreal Forest, Science, 339, 1615–1618, https://doi.org/10.1126/science.1231923, 2013.

Cotrufo, M. F., Ranalli, M. G., Haddix, M. L., Six, J., and Lugato, E.: Soil carbon storage informed by particulate and mineral-associated organic matter, Nat. Geosci., 12, 989–994, https://doi.org/10.1038/s41561-019-0484-6, 2019.

Fairbairn, L., Rezanezhad, F., Gharasoo, M., Parsons, C. T., Macrae, M. L., Slowinski, S., and Van Cappellen, P.: Relationship between soil CO_2 fluxes and soil moisture: Anaerobic sources explain fluxes at high water content, Geoderma, 434, 116493, https://doi.org/10.1016/j.geoderma.2023.116493, 2023.

Fernandez-Ugalde, O., Scarpa, S., Orgiazzi, A., Panagos, P., Van Liedekerke, M., Marechal, A., and Jones, A.: LUCAS 2018 soil module: presentation of dataset and results (No. JRC129926), Publications Office of the European Union, Luxembourg, https://doi.org/10.2760/215013, 2022.

Fiedler, S.: In Situ Long-Term-Measurement of Redox Potential in Redoximorphic Soils, Redox: Fundamentals, Processes and Applications, edited by: Schüring, J., Schulz, H. D., Fischer, W. R., Böttcher, J., and Duijnisveld, W. H. M., Springer,

Berlin, Heidelberg, 81–94, https://doi.org/10.1007/978-3-662-04080-5_7, 2000.

Fiedler, S., Vepraskas, M. J., and Richardson, J. L.: Soil Redox Potential: Importance, Field Measurements, and Observations, Advances in Agronomy, edited by: Sparks, D. L., Academic Press, 1–54, https://doi.org/10.1016/S0065-2113(06)94001-2, 2007.

Ghezzehei, T. A., Sulman, B., Arnold, C. L., Bogie, N. A., and Berhe, A. A.: On the role of soil water retention characteristic on aerobic microbial respiration, Biogeosciences, 16, 1187–1209, https://doi.org/10.5194/bg-16-1187-2019, 2019.

Ginn, B., Meile, C., Wilmoth, J., Tang, Y., and Thompson, A.: Rapid Iron Reduction Rates Are Stimulated by High-Amplitude Redox Fluctuations in a Tropical Forest Soil, Environ. Sci. Technol. 51, 3250–3259, 2017.

Goffin, S., Wylock, C., Haut, B., Maier, M., Longdoz, B., and Aubinet, M.: Modeling soil CO_2 production and transport to investigate the intra-day variability of surface efflux and soil CO_2 concentration measurements in a Scots Pine Forest (*Pinus Sylvestris*, L.), Plant Soil, 390, 195–211, https://doi.org/10.1007/s11104-015-2381-0, 2015.

Greenway, H., Armstrong, W., and Colmer, T. D.: Conditions Leading to High CO_2 (> 5 kPa) in Waterlogged–Flooded Soils and Possible Effects on Root Growth and Metabolism, Ann. Bot.-London, 98, 9–32, https://doi.org/10.1093/aob/mcl076, 2006.

Grybos, M., Davranche, M., Gruau, G., Petitjean, P., and Pédrot, M.: Increasing pH drives organic matter solubilization from wetland soils under reducing conditions, Geoderma, 154, 13–19, https://doi.org/10.1016/j.geoderma.2009.09.001, 2009.

Hakala, K., Keskitalo, M., Eriksson, C., and Pitkänen, T.: Nutrient uptake and biomass accumulation for eleven different field crops, Agr. Food Sci., 18, 366–387, 2009.

Hanke, A., Cerli, C., Muhr, J., Borken, W., and Kalbitz, K.: Redox control on carbon mineralization and dissolved organic matter along a chronosequence of paddy soils, Eur. J. Soil Sci., 64, 476–487, https://doi.org/10.1111/ejss.12042, 2013.

Hanson, P. J., Edwards, N. T., Garten, C. T., and Andrews, J. A.: Separating root and soil microbial contributions to soil respiration: A review of methods and observations, Biogeochemistry, 48, 115–146, https://doi.org/10.1023/A:1006244819642, 2000.

Heikkinen, J., Ketoja, E., Nuutinen, V., and Regina, K.: Declining trend of carbon in Finnish cropland soils in 1974–2009, Glob. Change Biol., 19, 1456–1469, https://doi.org/10.1111/gcb.12137, 2013.

Heikkinen, J., Keskinen, R., Kostensalo, J., and Nuutinen, V.: Climate change induces carbon loss of arable mineral soils in boreal conditions, Glob. Change Biol., 28, 3960–3973, https://doi.org/10.1111/gcb.16164, 2022.

Heimsch, L., Vira, J., Fer, I., Vekuri, H., Tuovinen, J.-P., Lohila, A., Liski, J., and Kulmala, L.: Impact of weather and management practices on greenhouse gas flux dynamics on an agricultural grassland in Southern Finland, Agr. Ecosyst. Environ., 374, 109179, https://doi.org/10.1016/j.agee.2024.109179, 2024.

Hill, A. G., Bishop, E., Coles, L. E., McLauchlan, E. J., Meddle, D. W., Pater, M. J., Watson, C. A., and Whalley, C.: Standardised General Method for the Determination of Iron with 1,10-Phenantrhroline, Analyst, 103, 391–396, 1978.

Hirsch, A. I., Trumbore, S. E., and Goulden, M. L.: The surface CO_2 gradient and pore-space storage flux in a high-porosity litter layer, Tellus B, 56, 312–321, https://doi.org/10.3402/tellusb.v56i4.16449, 2004.

Huang, W. and Hall, S. J.: Elevated moisture stimulates carbon loss from mineral soils by releasing protected organic matter, Nat. Commun., 8, 1774, https://doi.org/10.1038/s41467-017-01998-z, 2017.

Huang, W., Ye, C., Hockaday, W. C., and Hall, S. J.: Trade-offs in soil carbon protection mechanisms under aerobic and anaerobic conditions, Glob. Change Biol., 26, 3726–3737, https://doi.org/10.1111/gcb.15100, 2020.

Huang, W., Wang, K., Ye, C., Hockaday, W. C., Wang, G., and Hall, S. J.: High carbon losses from oxygen-limited soils challenge biogeochemical theory and model assumptions, Glob. Change Biol., 27, 6166–6180, https://doi.org/10.1111/gcb.15867, 2021.

IPCC: Sections 2–3, Climate Change 2023: Synthesis Report., Contribution of Working Groups I, II and III to the Sixth Assessment Report of the Intergovernmental Panel on Climate Change, edited by: Core Writing Team, Lee, H., and Romero, J., IPCC, Geneva, Switzerland, 184 pp., https://doi.org/10.59327/IPCC/AR6-9789291691647, 2023.

Ito, A. and Wagai, R.: Global distribution of clay-size minerals on land surface for biogeochemical and climatological studies, Sci. Data, 4, 170103, https://doi.org/10.1038/sdata.2017.103, 2017.

Jakobsen, P., Patrick, W. H. J., and Williams, B. G.: Sulfide and methane formation in soils and sediments, Soil Sci., 132, 279–287, 1981.

Jeanneau, L., Buysse, P., Denis, M., Gruau, G., Petitjean, P., Jaffrézic, A., Flechard, C., and Viaud, V.: Water Table Dynamics Control Carbon Losses from the Destabilization of Soil Organic Matter in a Small, Lowland Agricultural Catchment, Soil Syst., 4, 2, https://doi.org/10.3390/soilsystems4010002, 2020.

Jian, J., Du, X., Reiter, M. S., and Stewart, R. D.: A meta-analysis of global cropland soil carbon changes due to cover cropping, Soil Biol. Biochem., 143, 107735, https://doi.org/10.1016/j.soilbio.2020.107735, 2020.

Kaiser, K. and Guggenberger, G.: Mineral surfaces and soil organic matter, Eur. J. Soil Sci., 54, 219–236, 2003).

Kätterer, T., Reichstein, M., Andrén, O., and Lomander, A.: Temperature dependence of organic matter decomposition: a critical review using literature data analyzed with different models, Biol. Fert. Soils, 27, 258–262, https://doi.org/10.1007/s003740050430, 1998.

Kaye, J. P. and Quemada, M.: Using cover crops to mitigate and adapt to climate change. A review, Agron. Sustain. Dev., 37, 4, https://doi.org/10.1007/s13593-016-0410-x, 2017.

Keiluweit, M., Bougoure, J. J., Nico, P. S., Pett-Ridge, J., Weber, P. K., and Kleber, M.: Mineral protection of soil carbon counteracted by root exudates, Nat. Clim. Change, 5, 588–595, https://doi.org/10.1038/nclimate2580, 2015.

Keiluweit, M., Wanzek, T., Kleber, M., Nico, P., and Fendorf, S.: Anaerobic microsites have an unaccounted role in soil carbon stabilization, Nat. Commun., 8, 1771, https://doi.org/10.1038/s41467-017-01406-6, 2017.

Keskinen, R., Hillier, S., Liski, E., Nuutinen, V., Nyambura, M., and Tiljander, M.: Mineral composition and its relations to readily available element concentrations in cultivated soils of Finland, Acta Agr. Scand. B, 72, 751–760, https://doi.org/10.1080/09064710.2022.2075790, 2022.

Khan, I., Fahad, S., Wu, L., Zhou, W., Xu, P., Sun, Z., Salam, A., Imran, M., Jiang, M., Kuzyakov, Y., and Hu, R.: Labile organic matter intensifies phosphorous mobilization in paddy soils by microbial iron (III) reduction, Geoderma, 352, 185–196, https://doi.org/10.1016/j.geoderma.2019.06.011, 2019.

Kronberg, R.: A Schematic Illustration of the Soil Monolith Experiment Study Design, created in BioRender, https://BioRender.com/pg6cizz, last access: 12 June 2025.

Kronberg, R., Kanerva, S., Koskinen, M., Polvinen, T., Heinonsalo, J., and Pihlatie, M.: Controlled soil monolith experiment for studying the effects of waterlogging on redox processes, Geoderma, 452, 117110, https://doi.org/10.1016/j.geoderma.2024.117110, 2024.

Kronberg, R. A. M., Koskinen, M., Polvinen, T., Leinonen, L., Viinikainen, A., and Pihlatie, M.: Supporting data: Temporary waterlogging alters CO_2 flux dynamics but not cumulative emissions in cultivated mineral soils, Zenodo [data set], https://doi.org/10.5281/zenodo.14438980, 2025.

Kuzyakov, Y.: Sources of CO_2 efflux from soil and review of partitioning methods, Soil Biol. Biochem., 38, 425–448, https://doi.org/10.1016/j.soilbio.2005.08.020, 2006.

Kuzyakov, Y., Friedel, J. K., and Stahr, K.: Review of mechanisms and quantification of priming effects, Soil Biol. Biochem., 32, 1485–1498, https://doi.org/10.1016/S0038-0717(00)00084-5, 2000.

Lavallee, J. M., Soong, J. L., and Cotrufo, M. F.: Conceptualizing soil organic matter into particulate and mineral-associated forms to address global change in the 21st century, Glob. Change Biol., 26, 261–273, https://doi.org/10.1111/gcb.14859, 2020.

Lemola, R., Uusitalo, R., Hyväluoma, J., Sarvi, M., and Turtola, E.: Suomen peltojen maalajit, multavuus ja fosforipitoisuus: Vuodet 1996–2000 ja 2005–2009, Luonnonvarakeskus, ISBN 978-952-326-558-5, 2018.

Liu, Y., Jia, B., Zhang, Y., Cui, H., and Li, X. G.: The Effect of Waterlogging on Soil Organic Carbon Decomposition Is Dependent on Its Biochemistry, J. Soil Sci. Plant Nut., 23, 4609–4619, https://doi.org/10.1007/s42729-023-01377-2, 2023.

Liu, Y., Wang, X., Wen, Y., Cai, H., Song, X., and Zhang, Z.: Effects of freeze–thaw cycles on soil greenhouse gas emissions: A systematic review, Environ. Res., 248, 118386, https://doi.org/10.1016/j.envres.2024.118386, 2024.

Lovley, D. R.: Dissimilatory Fe(III) and Mn(IV) reduction, Microbiol. Rev., 55, 259–287, https://doi.org/10.1128/mr.55.2.259-287.1991, 1991.

Luo, Y. and Zhou, X.: Soil Respiration and the Environment, Academic Press, London, UK, https://doi.org/10.1016/B978-0-12-088782-8.X5000-1, 2006.

Maier, M., Schack-Kirchner, H., Hildebrand, E. E., and Holst, J.: Pore-space CO_2 dynamics in a deep, well-aerated soil, Eur. J. Soil Sci., 61, 877–887, https://doi.org/10.1111/j.1365-2389.2010.01287.x, 2010.

Maier, M., Schack-Kirchner, H., Hildebrand, E. E., and Schindler, D.: Soil CO_2 efflux vs. soil respiration: Implications for flux models, Agr. Forest Meteorol., 151, 1723–1730, https://doi.org/10.1016/j.agrformet.2011.07.006, 2011.

Mattila, T. J. and Vihanto, N.: Agricultural limitations to soil carbon sequestration: Plant growth, microbial activity, and carbon stabilization, Agr. Ecosyst. Environ., 367, 108986, https://doi.org/10.1016/j.agee.2024.108986, 2024.

Moyano, F. E., Manzoni, S., and Chenu, C.: Responses of soil heterotrophic respiration to moisture availability: An exploration of processes and models, Soil Biol. Biochem., 59, 72–85, https://doi.org/10.1016/j.soilbio.2013.01.002, 2013.

Moyano, F. E., Vasilyeva, N., and Menichetti, L.: Diffusion limitations and Michaelis–Menten kinetics as drivers of combined temperature and moisture effects on carbon fluxes of mineral soils, Biogeosciences, 15, 5031–5045, https://doi.org/10.5194/bg-15-5031-2018, 2018.

Muhammad, I., Wang, J., Sainju, U. M., Zhang, S., Zhao, F., and Khan, A.: Cover cropping enhances soil microbial biomass and affects microbial community structure: A meta-analysis, Geoderma, 381, 114696, https://doi.org/10.1016/j.geoderma.2020.114696, 2021.

Mui, N. T., Zhou, M., Parsons, D., and Smith, R. W.: Aerenchyma Formation in Adventitious Roots of Tall Fescue and Cocksfoot under Waterlogged Conditions, Agronomy, 11, 2487, https://doi.org/10.3390/agronomy11122487, 2021.

Nevalainen, O., Niemitalo, O., Fer, I., Juntunen, A., Mattila, T., Koskela, O., Kukkamäki, J., Höckerstedt, L., Mäkelä, L., Jarva, P., Heimsch, L., Vekuri, H., Kulmala, L., Stam, Å., Kuusela, O., Gerin, S., Viskari, T., Vira, J., Hyväluoma, J., Tuovinen, J.-P., Lohila, A., Laurila, T., Heinonsalo, J., Aalto, T., Kunttu, I., and Liski, J.: Towards agricultural soil carbon monitoring, reporting, and verification through the Field Observatory Network (FiON), Geosci. Instrum. Method. Data Syst., 11, 93–109, https://doi.org/10.5194/gi-11-93-2022, 2022.

Pan, W., Kan, J., Inamdar, S., Chen, C., and Sparks, D.: Dissimilatory microbial iron reduction release DOC (dissolved organic carbon) from carbon-ferrihydrite association, Soil Biol. Biochem., 103, 232–240, https://doi.org/10.1016/j.soilbio.2016.08.026, 2016.

Pavelka, M., Acosta, M., Kiese, R., Altimir, N., Brümmer, C., Crill, P., Darenova, E., Fuß, R., Gielen, B., Graf, A., Klemedtsson, L., Lohila, A., Longdoz, B., Lindroth, A., Nilsson, M., Jiménez, S. M., Merbold, L., Montagnani, L., Peichl, M., Pihlatie, M., Pumpanen, J., Ortiz, P. S., Silvennoinen, H., Skiba, U., Vestin, P., Weslien, P., Janous, D., and Kutsch, W.: Standardisation of chamber technique for CO_2, N_2O and CH_4 fluxes measurements from terrestrial ecosystems, Int. Agrophys., 32, 569–587, https://doi.org/10.1515/intag-2017-0045, 2018.

Peters, V. and Conrad, R.: Sequential reduction processes and initiation of CH_4 production upon flooding of oxic upland soils, Soil Biol. Biochem., 28, 371–382, https://doi.org/10.1016/0038-0717(95)00146-8, 1996.

Pinheiro, J. and Bates, D.: R Core Team: nlme: Linear and Nonlinear Mixed Effects Models. R package version 3.1-164, https://cran.r-project.org/web/packages/nlme/index.html (last access: 9 April 2026), 2023.

Poeplau, C., Aronsson, H., Myrbeck, Å., and Kätterer, T.: Effect of perennial ryegrass cover crop on soil organic carbon stocks in southern Sweden, Geoderma Reg., 4, 126–133, https://doi.org/10.1016/j.geodrs.2015.01.004, 2015.

Poeplau, C. and Don, A.: Carbon sequestration in agricultural soils via cultivation of cover crops – A meta-analysis, Agr. Ecosyst. Environ., 200, 33–41, https://doi.org/10.1016/j.agee.2014.10.024, 2015.

Ponnamperuma, F. N.: Chemical kinetics of wetland rice soils relative to soil fertility, Wetland Soils: Characterization, Classification, and Utilization, IRRI, 71–89, ISBN 971-104-139-1, 1985.

Possinger, A. R., Bailey, S. W., Inagaki, T. M., Kögel-Knabner, I., Dynes, J. J., Arthur, Z. A., and Lehmann, J.: Organo-mineral interactions and soil carbon mineralizability with variable saturation cycle frequency, Geoderma, 375, 114483, https://doi.org/10.1016/j.geoderma.2020.114483, 2020.

Raich, J. W. and Schlesinger, W. H.: The global carbon dioxide flux in soil respiration and its relationship to vegetation and climate, Tellus B, 44, 81–99, https://doi.org/10.1034/j.1600-0889.1992.t01-1-00001.x, 1992.

Rasmussen, C., Heckman, K., Wieder, W. R., Keiluweit, M., Lawrence, C. R., Berhe, A. A., Blankinship, J. C., Crow, S. E., Druhan, J. L., Hicks Pries, C. E., Marin-Spiotta, E., Plante, A. F., Schädel, C., Schimel, J. P., Sierra, C. A., Thompson, A., and Wagai, R.: Beyond clay: Towards an improved set of variables for predicting soil organic matter content, Biogeochemistry, 137, 297–306, https://doi.org/10.1007/s10533-018-0424-3, 2018.

R Core Team: R: A Language and Environment for Statistical Computing. R Foundation for Statistical Computing, https://www.R-project.org/ (last access: 9 April 2026), 2025.

Ruosteenoja, K. and Jylhä, K.: Projected climate change in Finland during the 21st century calculated from CMIP6 model simulations, Geophysica, 56, 39–69, 2022.

Russell, V. L.: Estimated Marginal Means, aka Least-Squares Means, R package version 1.8.5, https://CRAN.R-project.org/package=emmean (last access: 9 April 2026), 2023.

Ryan, M. G. and Law, B. E.: Interpreting, measuring, and modeling soil respiration, Biogeochemistry, 73, 3–27, https://doi.org/10.1007/s10533-004-5167-7, 2005.

Salonen, A.-R., de Goede, R., Creamer, R., Heinonsalo, J., and Soinne, H.: Soil organic carbon fractions and storage potential in Finnish arable soils, Eur. J. Soil Sci., 75, e13527, https://doi.org/10.1111/ejss.13527, 2024.

Sánchez-Cañete, E. P., Barron-Gafford, G. A., and Chorover, J.: A considerable fraction of soil-respired CO_2 is not emitted directly to the atmosphere, Sci. Rep.-UK, 8, 13518, https://doi.org/10.1038/s41598-018-29803-x, 2018.

Sigg, L.: Redox Potential Measurements in Natural Waters: Significance, Concepts and Problems, Redox: Fundamentals, Processes and Applications, edited by: Schüring, J., Schulz, H. D., Fischer, W. R., Böttcher, J., and Duijnisveld, W. H. M., Springer, 81–94, https://doi.org/10.1007/978-3-662-04080-5_7, 2000.

Sippola, J.: Mineral composition and its relation to texture and to some chemical properties in Finnish subsoils, Ann. Agric. Fenn., 13, 169–234, 1974.

Snoeyenbos-West, O. L., Nevin, K. P., Anderson, R. T., and Lovley, D. R.: Enrichment of Geobacter Species in Response to Stimulation of Fe(III) Reduction in Sandy Aquifer Sediments, Microb. Ecol., 39, 153–167, https://doi.org/10.1007/s002480000018, 2000.

Stumm, W.: Aquatic Chemistry: Chemical Equilibria and Rates in Natural Waters, John Wiley and Sons, Incorporated, http://ebookcentral.proquest.com/lib/helsinki-ebooks/detail.action?docID=7103403, 1995.

Sulman, B. N., Phillips, R. P., Oishi, A. C., Shevliakova, E., and Pacala, S. W.: Microbe-driven turnover offsets mineral-mediated storage of soil carbon under elevated CO_2, Nat. Clim. Change, 4, 1099–1102, https://doi.org/10.1038/nclimate2436, 2014.

Tautges, N. E., Chiartas, J. L., Gaudin, A. C. M., O'Geen, A. T., Herrera, I., and Scow, K. M.: Deep soil inventories reveal that impacts of cover crops and compost on soil carbon sequestration differ in surface and subsurface soils, Glob. Change Biol., 25, 3753–3766, https://doi.org/10.1111/gcb.14762, 2019.

Tete, E., Viaud, V., and Walter, C.: Organic carbon and nitrogen mineralization in a poorly-drained mineral soil under transient waterlogged conditions: an incubation experiment, Eur. J. Soil Sci., 66, 427–437, https://doi.org/10.1111/ejss.12234, 2015.

Torn, M. S., Trumbore, S. E., Chadwick, O. A., Vitousek, P. M., and Hendricks, D. M.: Mineral control of soil organic carbon storage and turnover, Nature, 389, 170–173, https://doi.org/10.1038/38260, 1997.

Uusitalo, R., Ylivainio, K., Hyväluoma, J., Rasa, K., Kaseva, J., Nylund, P., Pietola, L., and Turtola, E.: The effects of gypsum on the transfer of phosphorus and other nutrients through clay soil monoliths, Agr. Food Sci., 21, 260–278, https://doi.org/10.23986/afsci.4855, 2012.

Venables, W. N. and Ripley, B. D.: Random and Mixed Effects, Modern Applied Statistics with S, edited by: Venables, W. N. and Ripley, B. D., Springer, New York, 271–300, https://doi.org/10.1007/978-0-387-21706-2_10, 2002.

Vet, R., Artz, R. S., Carou, S., Shaw, M., Ro, C.-U., Aas, W., Baker, A., Bowersox, V. C., Dentener, F., Galy-Lacaux, C., Hou, A., Pienaar, J. J., Gillett, R., Forti, M. C., Gromov, S., Hara, H., Khodzher, T., Mahowald, N. M., Nickovic, S., Rao, P. S. P., and Reid, N. W.: A global assessment of precipitation chemistry and deposition of sulfur, nitrogen, sea salt, base cations, organic acids, acidity and pH, and phosphorus. Atmos. Environ., 93, 3–100, https://doi.org/10.1016/j.atmosenv.2013.10.060, 2014.

Virtanen, S., Simojoki, A., Knuutila, O., and Yli-Halla, M.: Monolithic lysimeters as tools to investigate processes in acid sulphate soil, Agr. Water Manage., 127, 48–58, https://doi.org/10.1016/j.agwat.2013.05.013, 2013.

von Lützow, M., Kögel-Knabner, I., Ekschmitt, K., Flessa, H., Guggenberger, G., Matzner, E., and Marschner, B.: SOM fractionation methods: Relevance to functional pools and to stabilization mechanisms, Soil Biol. Biochem., 39, 2183–2207, https://doi.org/10.1016/j.soilbio.2007.03.007, 2007.

Wickland, K. P. and Neff, J. C.: Decomposition of soil organic matter from boreal black spruce forest: environmental and chemical controls, Biogeochemistry, 87, 29–47, https://doi.org/10.1007/s10533-007-9166-3, 2008.

Williams, M. D. and Oostrom, M.: Oxygenation of anoxic water in a fluctuating water table system: an experimental and numerical study, J. Hydrol., 230, 70–85, https://doi.org/10.1016/S0022-1694(00)00172-4, 2000.

Winkler, P., Kaiser, K., Jahn, R., Mikutta, R., Fiedler, S., Cerli, C., Kölbl, A., Schulz, S., Jankowska, M., Schloter, M., Müller-Niggemann, C., Schwark, L., Woche, S. K., Kümmel, S., Utami, S. R., and Kalbitz, K.: Tracing organic carbon and microbial community structure in mineralogically different soils exposed to redox fluctuations, Biogeochemistry, 143, 31–54, https://doi.org/10.1007/s10533-019-00548-7, 2019.

Yong, R. N., Mohamed, A. M. O., and Wang, B. W.: Influence of amorphous silica and iron hydroxide on interparticle action and soil surface properties, Can. Geotech. J., 29, 803–818 , 1992.

Zeileis, A. and Grothendieck, G.: zoo: S3 Infrastructure for Regular and Irregular Time Series, https://doi.org/10.48550/arXiv.math/0505527, 2005.

Zhao, Q., Dunham-Cheatham, S., Adhikari, D., Chen, C., Patel, A., Poulson, S. R., Obrist, D., Verburg, P. S. J., Wang, X., Roden, E. R., Thompson, A., and Yang, Y.: Oxidation of soil organic carbon during an anoxic-oxic transition, Geoderma, 377, 114584, https://doi.org/10.1016/j.geoderma.2020.114584, 2020.

Zheng, J., Thornton, P. E., Painter, S. L., Gu, B., Wullschleger, S. D., and Graham, D. E.: Modeling anaerobic soil organic carbon decomposition in Arctic polygon tundra: insights into soil geochemical influences on carbon mineralization, Biogeosciences, 16, 663–680, https://doi.org/10.5194/bg-16-663-2019, 2019.